

1 **Epigenetic memory of temperature sensed during somatic embryo** 2 **maturation in 2-year-old maritime pine trees**

3 4 **Short title: Epigenetic memory in pine trees**

5
6 J.-F. Trontin^{1§§}, M.D. Sow^{2‡}, A. Delaunay², I. Modesto³, C. Teyssier⁴, I. Reymond¹, F. Canlet⁵,
7 N. Boizot⁴, C. Le Metté⁴, A. Gibert², C. Chaparro⁶, C. Daviaud⁷, J. Tost⁷, C. Miguel³, M.-A.
8 Lelu-Walter⁴ and S. Maury^{2§}

9
10 ¹BioForBois, FCBA, Pôle Industrie Bois & Construction, Cestas, 33610, France.

11 ²P2e, Université d'Orléans, INRAE, EA 1207 USC 1328, 45067 Orléans, France.

12 ³Biosystems and Integrative Sciences Institute, Faculdade de Ciências, Universidade de Lisboa,
13 1749-016 Lisboa, Portugal.

14 ⁴BioForA, INRAE, ONF, UMR 0588, 45075 Orléans, France.

15 ⁵Sylviculture Avancée, FCBA, Pôle Ressources Forestières des Territoires, Cestas, 33610,
16 France.

17 ⁶IHPE, Université de Perpignan, UMR 5244, 66100, Perpignan, France.

18 ⁷Laboratory for Epigenetics and Environment, Centre National de Recherche en Génomique
19 Humaine, CEA - Institut de Biologie François Jacob, Université Paris Saclay, 91000 Evry,
20 France.

21
22 [§]Present address: BEF, INRAE, UR 1138, 54280 Champenoux, France.

23 [‡]Present address: GDEC, INRAE, UMR 1095, 63000 Clermont-Ferrand, France.

24 [§]Corresponding authors: stephane.maury@univ-orleans.fr; jean-francois.trontin@inrae.fr

25
26 **Key message:** Developmental and temperature-induced changes in the methylome of
27 maritime pine somatic embryos can be stably transmitted from the embryonic to the post-
28 embryonic phase.

29
30 **Keywords:** *Pinus pinaster*, somatic embryogenesis, memory, epigenetics, development,
31 heat/cold stress, DNA methylation, methylome, sequence capture bisulfite.

32 **Abstract**

33

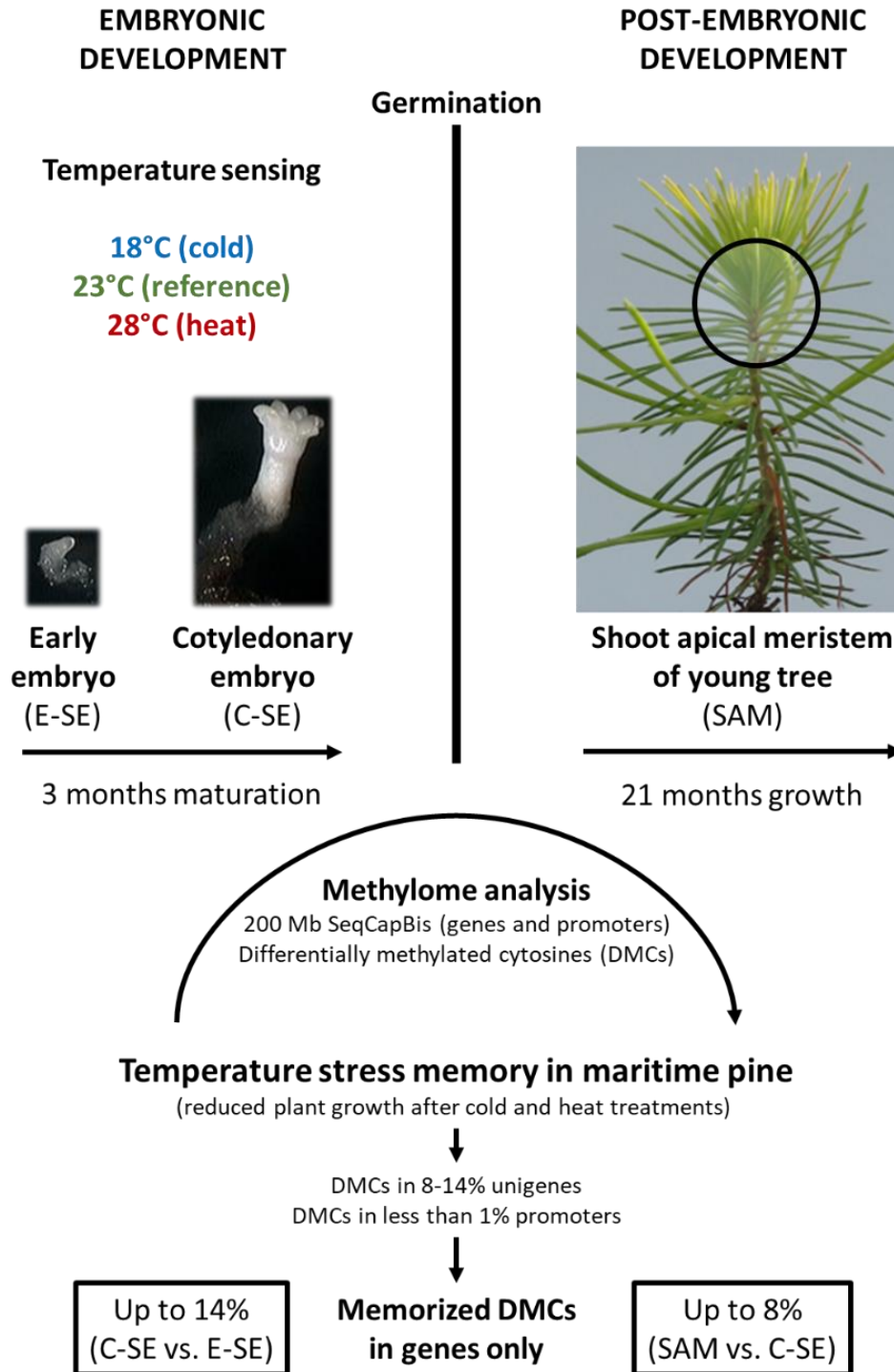
34 Embryogenesis is a brief but potentially critical phase in the tree life cycle for adaptive
35 phenotypic plasticity. Using somatic embryogenesis in maritime pine, we found that
36 temperature during the maturation phase affects embryo development and post-embryonic tree
37 growth for up to three years. We examined whether this somatic stress memory could stem from
38 temperature- and/or development-induced changes in DNA methylation. To do this, we
39 developed a 200 Mb custom sequence capture bisulfite analysis of genes and promoters to
40 identify differentially methylated cytosines (DMCs) between temperature treatments (18, 23,
41 and 28°C) and developmental stages (immature and cotyledonary embryos, shoot apical
42 meristem of 2-year-old plants) and investigate if these differences can be mitotically transmitted
43 from embryonic to post-embryonic development (epigenetic memory). We revealed a high
44 prevalence of temperature-induced DMCs in genes (8-14%) compared to promoters (less than
45 1%) in all 3 cytosine contexts. Developmental DMCs showed a comparable pattern but only in
46 the CG context, and with a high trend towards hypo-methylation, particularly in the promoters.
47 A high percentage of DMCs induced by developmental transitions were found memorized in
48 genes (up to 45-50%) and promoters (up to 90%). In contrast, temperature-induced memory
49 was lower and confined to genes after both embryonic (up to 14%) and post-embryonic
50 development (up to 8%). Using stringent criteria, we identified ten genes involved in defense
51 responses and adaptation, embryo development and chromatin regulation that are candidates
52 for the establishment of a persistent epigenetic memory of temperature sensed during embryo
53 maturation in maritime pine.

54

55 **Abbreviations:** C-SE: Cotyledonary Somatic Embryos; DMC: Differentially Methylated
56 Cytosine; d.m.: dry mass; E-SE: Early Somatic Embryos; f.m.: fresh mass; gDNA: genomic
57 DNA; HPLC: High-Performance Liquid Chromatography; JA: jasmonic acid; SAM: Shoot
58 Apical Meristem; SE: Somatic Embryo; SeqCapBis: Sequence Capture Bisulfite; SMP: Single
59 Methylation Polymorphism; 5mC: 5-methylcytosine.

60 **Graphical abstract**

61



62

63 INTRODUCTION

64

65 Due to their longevity, large size, and late reproductive phase, adaptability of trees to climate
66 change is a major concern. Projections all point towards a significant rise in temperature (Adak
67 et al. 2023) that will expose most forests to recurrent and/or more severe heat and drought
68 episodes (Plomion et al. 2016, Hammond et al. 2022). Such environmental stresses can have
69 adverse effects on tree capacity to produce seeds (Clark et al. 2021). In maritime pine (*Pinus*
70 *pinaster* Ait.) for example, a major plantation conifer in the Mediterranean basin, a strong
71 decline in seed production has been observed in French orchards since the late 2000s (Boivin
72 and Davi 2016). Biotic and abiotic factors are suspected, including temperature effects on
73 flowering and seed formation.

74 Embryogenesis is a short phase of the tree life cycle resulting in embryo formation within
75 seed. It occurs from the fertilized egg cell (zygotic embryo, ZE), and more rarely from
76 unfertilized reproductive or differentiated somatic cells (somatic embryo, SE). Somatic
77 embryogenesis is a promising vegetative propagation way for conifers (Klimaszewska et al.
78 2016). In these species, embryogenesis involves a cascade of auxin- and abscisic acid (ABA)-
79 mediated events, from pro-embryogenesis (ZE) to early and late embryogenesis (ZE, SE),
80 coordinating apical-basal and radial patterning (Trontin et al. 2016a, von Arnold et al. 2016).
81 Auxin-mediated cell fate decisions result in early delineation of primary shoot (SAM) and root
82 (RAM) apical meristems followed by procambium at the early cotyledonary embryo stage
83 (Palovaara et al. 2010, Brunoni et al. 2019).

84 There is increasing evidence that post-embryonic meristems may have a fundamental role in
85 plant adaptation and memory as primary sensors of environmental stresses (Lämke and Bäurle
86 2017, Maury et al. 2019, Zhu et al. 2023). The same could apply to embryonic meristems and
87 any embryogenic cell (Castander-Olarieta et al. 2021, Trontin et al. 2021).

88 Besides genetics, plant adaptation may also operate through either adaptive phenotypic
89 plasticity (i.e., the ability of a genotype to express different phenotypes), or robustness (when
90 a genotype shows a rather stable phenotype). These processes could support rapid evolutionary
91 changes and acclimation of plants (Nicotra et al. 2010) and are thought to involve epigenetic
92 factors affecting the expression of genes, but not their nucleotide sequence (Maeji and
93 Nishimura 2018, Zhu et al. 2023). Such changes can be reversibly imprinted in the genome at
94 a much higher rate than genetic mutations (Sow et al. 2018) through development (e.g., bud
95 break, Conde et al. 2017; dormancy, Kumar et al. 2016; embryogenesis, Markulin et al. 2021;
96 aging, Li et al. 2023) and environmental effects (e.g., drought, Jacques et al. 2021; heat, Perella

97 et al. 2022). They are mostly transient modifications allowing the resetting of expression
98 patterns at key developmental stages and continuous adaptation to new conditions (Hemenway
99 and Gehring 2023). Part of these changes can be stably maintained by cell division and support
100 the neoformation of adapted organs (Maury et al. 2019). Epigenetic changes can even promote
101 genetic variation leading to local adaptation (Sáez-Laguna et al. 2014, Platt et al. 2015,
102 Alakärppä et al. 2018). As SAM alternately produce vegetative and sexual organs, any stable
103 (epi)genetic modification of meristematic cells could be transmitted to gametes and progenies
104 (Hofmeister et al. 2020).

105 Somatic stress memory has been reported in annuals (Jacques et al. 2021, Zhu et al. 2023)
106 and perennials (de Freitas Guedes et al. 2018, Tan 2023). Current evidence points to synergistic
107 control by epigenetic and transcription factors (Liu et al. 2021, Gao et al. 2022b) that could be
108 critically expressed in meristems (Birnbaum and Roudier 2017, Maury et al. 2019), especially
109 in the case of thermomorphogenesis (Zhu et al. 2023). A memory of temperature during
110 embryogenesis with long-lasting effects was reported in Norway spruce (Johnsen et al. 2005,
111 Kvaalen and Johnsen 2008, Skrøppa 2022). Genetic selection has been ruled out (Besnard et al.
112 2008) and evidence for an epigenetic control emerged from transcriptomics (Yakovlev et al.
113 2011, 2014) and profiling of small RNAs (Yakovlev et al. 2010, 2020, Yakovlev and Fossdal
114 2017).

115 DNA methylation has a pivotal role in epigenetics and has been the focus of numerous
116 studies to explore inheritable phenotypic variation (Seymour and Becker 2017). It
117 predominantly occurs in plants at cytosine sites as 5-methylcytosine (5mC) in the CG, CHG
118 (H: A, C, or T) and CHH contexts (Stroud et al. 2014, Zhang et al. 2018). Different DNA
119 methyltransferase classes are involved in methylation maintenance at these sites (MET1,
120 CMT3, and CMT2, respectively) while *de novo* methylation is mediated by DRM1/2 through
121 RNA-directed DNA methylation (RdDM) involving 24-nucleotide short interfering RNAs
122 (siRNAs, Matzke and Mosher 2014). There are both functional similarities and divergence of
123 these pathways in higher plants (Ausin et al. 2016, Niu et al. 2022, Li et al. 2023) that may
124 explain different DNA methylation patterns in some groups (e.g., higher levels in all 3 contexts
125 for gymnosperms).

126 Cytosine (de)methylation can occur at high rate in the genome (Yao et al. 2021) and has long
127 been associated in angiosperms with biological processes, cellular functions and regulation of
128 gene expression during embryonic (Ji et al. 2019, Chen et al. 2020, Wójcikowska et al. 2020,
129 Markulin et al. 2021) and post-embryonic development (Zhang et al. 2018), symbiotic
130 interactions (Vigneaud et al. 2023), stress responses and somatic memory (Zhang et al. 2018,

131 Le Gac et al. 2018, Liu and He 2020, Rajpal et al. 2022). Similar essential roles are anticipated
132 for gymnosperms with also a focus on genome stability as these species typically show much
133 larger and heavily methylated genomes because of high content in transposable elements (Ausin
134 et al. 2016, Niu et al. 2022).

135 In maritime pine, transcriptomics suggested that epigenetic reprogramming is occurring
136 during embryogenesis (de Vega-Bartol et al. 2013, Rodrigues et al. 2018, 2019). There is
137 evidence for both methylation maintenance during early embryogenesis and *de novo* RdDM
138 towards the late stages. Global DNA methylation changes or methylation-sensitive
139 amplification polymorphisms have been detected during somatic embryogenesis in conifers
140 (Miguel et al. 2016) and associated with embryo developmental stages (Teyssier et al. 2014) or
141 maturation ability (Klimaszewska et al. 2009). Global changes were also observed in pine
142 following temperature sensing during SE initiation or maturation suggesting that DNA
143 methylation could contribute to the establishment of an epigenetic stress memory (Castander-
144 Olarieta et al. 2020, Pereira et al. 2021). Despite increasing availability of genomic resources
145 in trees (Plomion et al. 2016, Sterck et al. 2022), evidence for temperature effect on genes
146 involved in DNA methylation (Yakovlev et al. 2016), and the possibility for bisulfite
147 sequencing, it is still unknown what is the extent of 5mC imprinting during conifer
148 embryogenesis as a result of both developmental transition and temperature sensing effects.

149 In this work, we used somatic embryogenesis as an *in vitro* process mimicking zygotic
150 embryogenesis in maritime pine (Morel et al. 2014a, Trontin et al. 2016b, Rodrigues et al. 2019)
151 to investigate whether developmental transitions and temperature during SE maturation could
152 induce changes in phenotype and methylome. We produced early (E-SE) and cotyledonary (C-
153 SE) embryos at 18, 23 (reference) and 28°C and further regenerated somatic plants (Fig. 1A).
154 We used available pine genomic resources to perform a targeted bisulfite sequencing of genes
155 and promoters (Fig. 1B) in E-SE, C-SE (direct development or temperature effects) and the
156 SAM of young trees (remaining, delayed effects). We found large sets of genes but fewer
157 promoters containing differentially methylated cytosines (DMCs) induced by embryonic
158 (comparing C-SE and E-SE) and post-embryonic (SAM vs. C-SE) development or temperature
159 in E-SE, C-SE and SAM in response to cold (18 vs. 23°C) or heat (28 vs. 23°C). A significant
160 part of development- (in genes and promoters) but also temperature-induced DMCs (in genes
161 only) were mitotically transmitted from the embryonic to the post-embryonic phase. We could
162 demonstrate both developmental and stress epigenetic memory established during
163 embryogenesis in maritime pine.

164 MATERIAL AND METHODS

165

166 Plant material, experimental design, and sampling

167 We investigated one cryopreserved *P. pinaster* embryogenic line (PN519) initiated in 1999
168 from an immature seed (G0.4304*G0.4301; pedigree: Landes Forest, France). It is a gold
169 genotype to study embryo development (Lelu-Walter et al. 2016, Trontin et al. 2016b, Llebrés
170 et al. 2018).

171 PN519 was subjected to three temperature treatments (18, 23, 28°C; Fig. 1A) during the
172 maturation step enabling the development of immature E-SE into C-SE. 23°C is the reference
173 temperature used during somatic embryogenesis in maritime pine (Trontin et al. 2016b). To
174 study the effect on DNA methylation at lower (18°C) or higher (28°C) maturation temperature
175 than the reference (23°C), we sampled and characterized three types of biological materials: i)
176 E-SE after 1 week maturation; ii) C-SE after at least 12 weeks maturation; and iii) SAM
177 collected from 21-month-old plants. The production process of this plant material is presented
178 in Fig. 1A.

179 For each type of embryonic (E-SE, C-SE) or post-embryonic (SAM) material and
180 temperature treatment combination, 3-5 biological replicates were made, immediately frozen in
181 liquid nitrogen and stored at -80°C until processing. E-SE sample (400 mg fresh mass, f.m.)
182 consisted of multiple immature embryos attached to remaining embryogenic tissue. C-SE
183 sample (200 mg f.m.) included 231-306 single embryos separated from the residual tissue. SAM
184 sample (2-4 mg f.m.) resulted from the dissection of the apical meristem of a single shoot apex.
185

186 Culture of somatic embryos and plants

187 Reactivation from the cryopreserved stock, multiplication, and maturation of PN519 were
188 performed in Petri dishes (94x16 mm) containing 23.5 mL semi-solid mLV basal medium
189 (Litvay et al. 1985, Klimaszewska et al. 2001) and closed by cling film (2 rounds). Cultures
190 were incubated at a selected temperature ($\pm 1^\circ\text{C}$) in darkness (TC175S, Aqualytic, Dortmund,
191 Germany).

192 Embryogenic tissues were thawed at 37°C, drained and plated on filter paper (Whatman N°2,
193 70 mm), then placed on mLV supplemented with 0.5 M sucrose, 2 μM 2,4-
194 dichlorophenoxyacetic acid (Sigma-Aldrich/Merck KGaA, Darmstadt, Germany), 1 μM 6-
195 benzyladenine (Duchefa Biochemie, Haarlem, The Netherlands) and solidified with 4.5 g/L
196 gellan gum (HP696, Kalys, Bernin, France). After 24 h, the filters supporting cells were
197 transferred to the same reactivation medium, but containing 0.3 M sucrose. After 48 h, the cells

198 were scraped off the filter and transferred to the same medium with standard sucrose (0.09 M)
199 and gellan gum concentrations (3 g/L Gelrite, Duchefa Biochemie) for multiplication. From 2
200 weeks after thawing, the reactivated line was weekly subcultured on multiplication medium to
201 promote rapid growth. When propagating easily, embryogenic tissue was suspended in liquid
202 maturation medium (mLV supplemented with 0.2 M sucrose, 80 μ M ABA, Ecochem, China),
203 and distributed on filter paper (Whatman N^o2, 70 mm) at a cell density of 50-300 mg f.m./filter.
204 The filter was then placed onto maturation medium solidified with high gellan gum (9 g/L
205 Gelrite) and subcultured once on fresh medium after 4 weeks. At 23°C, C-SE development
206 typically occurs after 10-14 weeks (Morel et al. 2014a).

207 C-SE were collected under the binocular and stored in darkness at 4°C on a modified mDCR
208 medium (Gupta and Durzan 1985) without plant growth regulator, 0.175 M sucrose and 9 g/L
209 gellan gum (Gelrite, Duchefa Biochemie). After 4-5 months, C-SEs were germinated (N =
210 120/condition) on mDCR containing 58 mM sucrose and 4.6 g/L gellan gum (4 g/L Gelrite,
211 Duchefa Biochemie; 0.6 g/L HP696, Kalys). After 3 weeks at 23°C, a subset of viable embryos
212 (N = 96/condition) were transferred in 8-ml miniplugs (15% peat, 85% coco fiber, Preforma
213 plug trays, ViVi, Mijlweg, The Netherlands) and cultivated in a growth room (1 month, 23°C),
214 then in the greenhouse (3 months, 25°C) until full acclimatization. Young trees were
215 transplanted in horticultural substrate at age 4 (110 ml container) and 15 months (one-l pot) and
216 further grown in the greenhouse until age 25 months. At this time, a subset of trees (N =
217 45/condition) were transferred to the nursery until planting in fall at age 31 months (Oct. 2018).
218 The field trial consists of 3 blocks with a fully randomized design (N = 5 trees/condition within
219 each block).

220

221 **Phenotypic characterization**

222 Embryogenic cultures matured at the 3 temperatures were characterized (Mat. S1) through
223 macro- and micro-morphological qualitative observations (behavior of cultures, overall time
224 required to produce C-SE) and quantitative measurements (embryo yield, mass, size, and
225 morphology).

226 Embryo yield was calculated as the number of C-SE harvested per gram f.m. embryogenic
227 tissue matured. It was estimated after 12-18 weeks maturation depending on temperature
228 treatment (see Results). Mean C-SE f.m. (mg) was estimated from the 5 samples collected for
229 DNA methylation analysis by dividing the total mass of each sample (ca. 200 mg) by the
230 number of embryos harvested. Embryo size (mm) and morphology were investigated based on
231 pictures (N = 60/condition) analyzed with the Acrobat Reader DC (Adobe) measurement tool.

232 We assessed total embryo length (from the hypocotyl base to the tip of the largest cotyledon),
233 cotyledon ring length (from the insertion point on the hypocotyl to the tip of the largest
234 cotyledon), hypocotyl length (from the root pole base to the insertion point of the cotyledon
235 ring) and width (just below insertion point of the cotyledon ring), and the number of cotyledons.

236 We also investigated the delayed effect of maturation temperature on C-SE development,
237 from germination (viability and germination rates) to plant survival and growth (height, height
238 increase, terminal bud elongation). Embryo viability and germination rates were checked after
239 3 weeks, i.e., just before transfer to miniplugs. Viability rate was calculated as the percentage
240 of viable C-SEs with elongated hypocotyl and cotyledons on germination medium. Germination
241 rate is the percentage of viable C-SEs with root development (checked under the binocular).

242 Plant survival in the greenhouse conditions was recorded at ages 5, 8, and 15 months after
243 germination and then yearly in the field (2019, 2020, 2021). Plant height (cm) was measured at
244 ages 8, 15, 36, and 65 months. Relative height increase (%) was calculated as
245 $(H_n - H_{n-1}) / H_{n-1} * 100$ with H_n the total height observed at measurement n. To characterize bud
246 “break” during early spring, which is an indefinite, temperature-dependent process in maritime
247 pine (from bud swelling to elongating bud and prickly shoot), we monitored the terminal bud
248 length (from main plant axis) in late March and early May during the spring of 2019 and 2021.
249 Relative increase in length (%) was calculated as $(L_n - L_{n-1}) / L_{n-1} * 100$ with L_n the length at
250 measurement n.

251

252 **Quantification of soluble carbohydrates and starch**

253 E-SE and C-SE samples (n = 5 biological replicates) were lyophilized and ground into fine
254 powder using a MM400 Retsch mixer Mill. Each sample (4-20 mg dry mass, d.m.) was
255 extracted three times at 85°C in 1 mL ethanol:water (80:20, v/v) for soluble carbohydrates and
256 starch following Bonhomme et al. (2010) modified by Gautier et al. (2019). Mannitol was added
257 in the extracts as an internal standard (0.25 mg/mL). Pooled, purified, and dried supernatants
258 were suspended in 250 µL ultrapure water and centrifuged before analyses by HPLC (see
259 Gautier et al. 2019). Soluble carbohydrates were identified by co-elution with standards and
260 quantified from the calibration curves (mg carbohydrates/g d.m, Mat. S1). From the resulting
261 pellets, starch content was quantified in glucose equivalents (mg glucose/g d.m., Mat. S1) after
262 hydrolysis with amyloglucosidase (Morel et al. 2014a). Each sample was assayed one (soluble
263 carbohydrates) or two times (starch).

264 **Total protein assay**

265 Total protein extracts were prepared in five replicates for each sample type from frozen material
266 (25-50 mg f.m.) according to Morel et al. (2014a). Protein concentration ($\mu\text{g}/\text{mg}$ f.m., Mat. S1)
267 was determined using the Bradford assay (1 time) with bovine serum albumin as a standard.

268

269 **DNA extraction and global DNA methylation percentages by HPLC**

270 Genomic DNA (gDNA) was extracted from E-SE (400 mg f.m.), C-SE (200 mg f.m.) and
271 individual SAM ($n = 3$ for each developmental stage and temperature condition; 27 samples
272 overall) using a CTAB protocol (Doyle and Doyle 1987) and was stored at -80°C . gDNA
273 quantity and quality were assessed using a NanoDrop spectrometer (Thermo Fisher Scientific,
274 Waltham, MA, USA). For estimating global DNA methylation, gDNA was enzymatically
275 hydrolyzed into nucleosides and analyzed by HPLC (Zhu et al. 2013, Genitoni et al. 2020).

276

277 **Sequence capture bisulfite for methylome analysis**

278 Designed probes are available in Mat. S2. An equimolar pool of $1 \mu\text{g}$ gDNA extracted from 3
279 biological samples was made for each developmental stage in each temperature treatment.
280 Bisulfite treatment and capture using our custom designed probes were made on these 9 types
281 of biological samples according to SeqCap Epi Target Enrichment System (SeqCap Epi
282 Developer XL Enrichment Kit) using Roche recommendations
283 ([https://sequencing.roche.com/content/dam/rochesequence/worldwide/resources/brochure-](https://sequencing.roche.com/content/dam/rochesequence/worldwide/resources/brochure-seqcap-epi-SEQ100146.pdf)
284 [seqcap-epi-SEQ100146.pdf](https://sequencing.roche.com/content/dam/rochesequence/worldwide/resources/brochure-seqcap-epi-SEQ100146.pdf)). Similar equimolar pools of $0.4 \mu\text{g}$ gDNA at ca. $20 \text{ ng}/\mu\text{L}$ were
285 used for sequencing at the CNRGH (Evry, France) with paired ends ($2 \times 150 \text{ bp}$) on an Illumina
286 HiSeq4000 platform following. Raw data were stored in FASTQ files with a minimal
287 theoretical coverage of 100X.

288 A Roche NimbleGen SeqCap EZ Design ([https://sequencing.roche.com/content/dam/rochesequence/worldwide/resources/brochure-seqcap-ez-prime-choice-probes-](https://sequencing.roche.com/content/dam/rochesequence/worldwide/resources/brochure-seqcap-ez-prime-choice-probes-SEQ100193.pdf)
289 [SEQ100193.pdf](https://sequencing.roche.com/content/dam/rochesequence/worldwide/resources/brochure-seqcap-ez-prime-choice-probes-SEQ100193.pdf))

290 of custom 200 Mb was performed by NimbleGen service using the 3
291 following supporting reference sequences and conditions (see Fig. 1B and Mat. S2 for details):

292 i) 866 *P. pinaster* gene models from Seoane-Zonjic et al. (2016) with the condition of covering
293 the whole gene body sequences, ii) 206,574 *P. pinaster* unigenes derived from Cañas et al.
294 (2017) with the conditions of covering the whole unigene (gene body) sequences if size is under
295 1,578 bp, and 789 bp in 5' and 3' for a total of 1,578 bp if unigene size is over or equal to 1,578
296 bp, and iii) 51,749 promoters from Pita v2.0 *Pinus taeda* genome

297 (<https://treegenesdb.org/FTP/Genomes/Pita/v2.0/>; Zimin et al. 2017) with the condition of
298 covering until 1,205 bp upstream to the transcription starting site (TSS).

299 The bioinformatic pipeline for methylome analysis was adapted from the ENCODE pipeline
300 (<https://www.encodeproject.org/wgbs/>) and installed on the Galaxy instance, accessible at
301 IHPE (<http://galaxy.univ-perp.fr/>, Perpignan, France) according to Sow et al. (2021) and Dugé
302 de Bernonville et al. (2022). Single Methylation Polymorphism (SMP) data were processed
303 against the 3 sets of supporting reference sequences (Fig. 1B) using the methylKit R package
304 (Akalin et al. 2012) to identify Differentially Methylated Cytosines (DMCs) with a minimum
305 coverage of 10X, differential methylation between two samples of at least 25% for all contexts
306 and a q -value < 0.01 . Gene annotation was achieved by similarity search using megaBLAST
307 alignments (BLAST+ BLASTN v2.10.1) against *Arabidopsis thaliana* genome v11 available
308 at TAIR database (<https://www.arabidopsis.org/>). Gene Ontology (GO) enrichment analysis of
309 methylated genes was performed using default parameters (see Mat. S3) of Metascape (Zhou
310 et al. 2019, <https://metascape.org/gp/index.html#/main/step1>).

311

312 **Statistical analyses of phenotypic data**

313 Biological data were analyzed using Statview 5.0 (SAS Institute Inc). Differences in means
314 (reported with 95% confidence limits) between temperature treatments for quantitative traits
315 were assessed by analysis of variance (ANOVA). Student-Newman-Keul's (SNK) post-hoc test
316 was used to identify differences between groups ($p < 0.05$) when ANOVA indicated significant
317 effects. Biochemical data were similarly assessed by one-way ANOVA and multiple
318 comparison of means with Tukey contrasts ($p < 0.05$) using the R version 3.3.2 (R Development
319 Core Team 2011, R: A Language and Environment for Statistical Computing. Vienna: R
320 Foundation for Statistical Computing). Statistical tests and p -values are indicated as
321 recommended by Wasserstein and Lazar (2016).

322 RESULTS

323

324 The maturation temperature affects biological and biochemical aspects of embryonic 325 development and post-embryonic growth

326 The first effect observed after only 1 week maturation of the PN519 line was the temperature-
327 dependent increase in cell proliferation (Fig. 1A, Fig. 2A). For high temperatures such as 28°C,
328 cell proliferation could be modulated by reducing inoculum density from 100 (standard) to 50
329 mg/filter (Fig. 2A). At these 2 plating densities, both lower (18°C) and higher temperature
330 (28°C) than the reference (23°C) significantly delayed embryo development (Table S1).

331 E-SE samples were produced at a high cell density in the 3 temperature conditions. In
332 contrast, C-SE samples were obtained at standard cell density at 18°C and 23°C and reduced
333 cell density at 28°C to avoid tissue overgrowth. Yields in C-SE were computed after 12-13
334 (23°C), 15-16 (28°C) or 17-18 weeks (18°C) maturation at the 3 selected cell densities to
335 produce E-SE and C-SE samples. They were the highest at 23°C (Fig. 2B). Despite downward
336 adjustment of cell density and/or extension of maturation time, embryo yields were lower at
337 28°C, and even more at 18°C.

338 The mean fresh mass of individual C-SE harvested for DNA methylation analysis
339 significantly increased ($p < 0.05$) with temperature, from 0.68 (18°C) to 0.83 mg (28°C) (Fig.
340 2C). The increase is greater between 28 and 23°C ($p < 0.01$) than between 23 and 18°C
341 ($p < 0.05$).

342 Significant effects of temperature on C-SE size (Fig. S1A) were detected for total length (p
343 = 0.0001), hypocotyl length, and width ($p < 0.0001$). Since ANOVA did not detect any effect
344 for cotyledon ring length, it can be deduced that it is mainly the hypocotyl that accounts for the
345 observed differences. Post-hoc SNK tests confirmed that hypocotyl size was significantly
346 reduced ($p < 0.01$) at 18°C compared to 23/28°C for both length (0.79 vs. 1.16 / 1.09 mm) and
347 width (0.59 vs. 0.67 / 0.70 mm). ANOVA also revealed a temperature effect on cotyledon
348 number ($p = 0.0008$). Embryos bore fewer cotyledons ($p < 0.01$) at 18°C (3.0) than at 23°C
349 (3.7) or 28°C (3.9).

350 Quantitative biochemical differences were detected between E-SE and C-SE (Fig. S1B), i.e.,
351 more proteins (Table 1, Mat. S1), sucrose, starch, and oligosaccharides of the raffinose family
352 (RFOs, raffinose, stachyose) in C-SE, but less glucose and fructose (Fig. S1B). In addition,
353 maturation temperature affected the content of starch and soluble carbohydrates in both E-SE
354 and C-SE (Fig. S1B). In E-SE, starch was higher at 18°C (47.4 mg/g d.m.) compared to 23 and
355 28°C (19.7-28.8 mg/g) and glucose increased as a function of temperature, from 131.4 mg/g

356 (18°C) to 199.0 mg/g (28°C). In C-SE, starch accumulated more efficiently at 23°C (127.2
357 mg/g) than at 18°C (103.9 mg/g) or 28°C (86.0 mg/g), and sucrose content was lower at 28°C
358 (99.5 vs. 121.3 mg/g).

359 The C-SE viability and germination rates were estimated after 4-5 months storage (Fig.
360 S1C). Despite the observed morphological and biochemical differences (Fig. 2C, S1A, S1B),
361 C-SE showed similar viability and germination rates when entering the post-embryonic phase
362 (3 weeks germination), whatever the maturation temperature. Viability rates were high and in
363 a narrow range 85-89%. Germination rates were lower and displayed a wider range (50-58%),
364 but differences were not significant. Similarly, we did not observe any major effect of
365 maturation temperature on plant survival after 5-, 8-, and 15-months (Table S2). A slightly
366 lower survival rate was observed after 15 months at 23°C (73%) compared to 18°C (81%) or
367 28°C (80%). However, the distribution of dead plants within the seedling trays was uneven and
368 points to undetected plant management issues. Furthermore, we noticed at age 15 some
369 substantial chlorosis of plants obtained from embryos matured at 18°C (intense) and 28°C
370 (moderate) as compared to 23°C (Fig. 2D). Accordingly, these two plant batches showed
371 significantly lower height at ages 8 and 15 months (Fig. 2E). This difference originated from
372 early stages of post-embryonic growth (before 8 months) since the three plant lots showed no
373 significant variation in relative height increase between 8 and 15 months (Fig. S1D), a period
374 that essentially matches spring shooting. Significant differences in growth were still detected
375 after field planting (Fig. 2E). Three years after germination, the 18°C plant batch showed a
376 lower average height. No significant difference could be detected after about 3 years of field
377 growth (age 65 months, Fig. S1E). However, the trial suffered from significant game damages
378 (35% of plants) during the first year. Similarly, we did not detect delayed effects when
379 considering terminal bud elongation during early spring of 2019 and 2021 (age 37-62 months,
380 Fig. 2F).

381 In summary, lower (18°C) or higher (28°C) temperature than the reference (23°C) during
382 embryo maturation adversely affects embryonic development and post-embryonic plant growth
383 up to 36 months following germination.

384 **Whole genome DNA methylation is more impacted by developmental transition than**
385 **temperature during embryo maturation**

386 To study DNA methylation in our biological material (E-SE, C-SE, SAM) following embryo
387 maturation at 18, 23 or 28°C (9 types of samples), we performed a global DNA methylation
388 analysis by HPLC and a custom methylome profiling using SeqCapBis (Fig. 1B).

389 Global DNA methylation values ranged from 15.1% (E-SE, 23°C) to 29.3% (C-SE, 23°C)
390 (Fig. S2A) with a significant developmental effect (ANOVA, $p = 0.013$). DNA methylation
391 levels were found lower in E-SE compared to C-SE ($p = 0.014$) with intermediate, not
392 significantly different values for SAM samples. No temperature effect was observed (ANOVA,
393 $p = 0.179$).

394 A capture probe design for a 200 Mb SeqCapBis of the *P. pinaster* methylome including
395 genes models (866), unigenes (206,574) and promoters (51,749) was used for DNA methylation
396 analysis (Fig. 1B, Mat. S2). Mapping coverage (Table S3) ranged from a mean of 19x
397 (promoters) to 57x (unigenes), and 235x (gene models). Considering unigenes and promoters,
398 cytosine methylation levels ranged from 65.0-71.6% (CG) to 55.6-58.5% (CHG), and 10.4-
399 20.7% (CHH) (Fig. S2B, Fig. S4). Unigenes display higher CG ($p = 0.035$) and lower CHH
400 methylation levels ($p = 0.009$) than promoters. Gene models and unigenes followed similar
401 methylation patterns in the 3 contexts (Fig. S3A, Fig. S4).

402 The number of cytosine positions that could be analyzed for Single Methylation
403 Polymorphisms (SMPs) is ascending from CG (0.13-0.99 million) to CHG (0.21-1.72) and
404 CHH (0.87-5.89) contexts, as expected due to their genomic frequency (Fig. 3A,B, Fig. S3C).
405 In line with the capture design (Fig. 1B), we found more SMPs in unigenes than promoters (6-
406 8 times, Fig. 3A,B) or gene models (30-40 times, Fig. 3A and Fig. S3C). Using SMP values,
407 correlations between samples (Fig. S5) were found higher for promoters (r up to 0.93 in CG,
408 0.88 in CHG, 0.78 in CHH) than for unigenes (r up to 0.88 in CHH, 0.86 in CG, 0.80 in CHG).
409 Hierarchical clustering of samples based on SMP occurrence (Fig. S2C and S3B) was quite
410 consistent with developmental stages in CHH (promoters, unigenes), CHG (unigenes,
411 promoters) and CG (promoters) contexts. E-SE generally cluster with SAM rather than C-SE
412 samples suggesting deep methylation rearrangements during development. In contrast, there
413 was no influence of the temperature treatments on the clustering.

414 **High prevalence of differentially methylated cytosines in genes compared to promoters,**
415 **especially in response to temperature**

416 Differentially Methylated Cytosines (DMCs) were identified in the 3 methylation contexts and
417 for the 3 designs (gene models, unigenes, and promoters) among temperature treatments for
418 cold (18 vs. 23°C) and heat effect (28 vs. 23°C), or among developmental stages at 23°C for
419 direct (E-SE vs. C-SE) and delayed effect (C-SE vs. SAM). DMCs were grouped into three
420 classes (Fig. S6): i) temperature-DMCs identified in E-SE or C-SE exposed to maturation
421 temperature (i.e., during embryonic development), ii) remaining temperature-DMCs identified
422 in plant SAM (i.e., after post-embryonic development) and iii) development-DMC identified
423 after embryonic (C-SE) or post-embryonic development (plant SAM). For genes (unigenes and
424 gene models), 3-11% of CG/CHG and only 1-5% of CHH SMP sites were in significant
425 temperature- and remaining temperature-DMCs in all conditions (Fig. 3C, Fig. S3D). A similar
426 pattern was observed for development-DMCs (6-11% of CG/CHG, and 2-5% of CHH SMP
427 sites). In contrast, for promoters (Fig. 3D), less than 0.1% of SMPs in all 3 contexts were in
428 temperature- and remaining temperature-DMCs while development-DMCs were also lower
429 than in genes for CG (< 0.1%) and CHG (< 1.3%), but similar in CHH (1.3-3.1%).

430 Temperature- and remaining temperature-DMCs in unigenes, gene models, and promoters
431 were similarly hyper- and hypo-methylated in all 3 contexts (Fig. S7). In contrast, both
432 embryonic and post-embryonic development-DMCs were found mostly hypo-methylated in
433 genes and even more in promoters, notably in CHH/CHG contexts (Fig. S7, Table 1).

434 About 25,000 out of the 206,574 unigenes (12%) had at least one temperature-, remaining
435 temperature- or development-DMC in each context (Fig. 4A,B). Filtering for more than 5
436 DMCs resulted in less than 3,000 (1.5%) unigenes in the CG context and 8,000-10,000 in the
437 CHG/CHH context (4-5%) considering both temperature (Fig. S8A, highest values for C-SE
438 under heat or cold in CHH) and development effects (Fig. S8B, similar numbers for embryonic
439 and post-embryonic development). GO enrichment analysis (see Mat. S3) showed that the main
440 molecular functions ($-\log_{10}(P) > 6$) of unigenes containing temperature-, remaining
441 temperature- or development-DMCs are related to primary (photosynthesis, polysaccharide
442 metabolism, glycolysis/gluconeogenesis, nucleobase-containing small molecule metabolic
443 process) or secondary metabolisms (phenylpropanoid metabolic process) and protein
444 autophosphorylation (see Fig. S9B for heat effect on C-SE, cold remaining effect on SAM and
445 post-embryonic developmental effect). Response to heat and other abiotic stresses (reactive
446 oxygen species, osmotic, etc.) were also well represented ($-\log_{10}(P) > 4$), especially for

447 temperature, but also development effects. In both cases molecular functions associated with
448 embryo and seedling development could be identified.

449 Regarding promoters, less than 200 out of the 51,749 promoters (0.4%) displayed
450 temperature- or remaining temperature-DMCs in each context, with highest values for C-SE
451 under heat (CHG/CHH) and the lowest for SAM, especially under heat in the 3 contexts (Fig.
452 4A). In contrast, development-DMC were found in up to 2,000-7,000 promoters (10 to 35 times
453 more, 4-14%), notably in the CHH context, with the highest number for post-embryonic
454 development (Fig. 4B). As previously observed for unigenes, GO enrichment analysis (Mat.
455 S3) confirmed for promoters molecular functions related to primary and secondary metabolic
456 processes as well as specific “response to temperature stimulus” for C-SE under heat (-
457 $\log_{10}(P)>4$) and, intriguingly, also post-embryonic developmental effects ($-\log_{10}(P)>6$, Fig.
458 S9A). In contrast, limited evidence for molecular functions associated with embryo or seedling
459 development was found in promoters.

460

461 **DMCs can be stably transmitted from the embryonic to the post-embryonic phase with higher**
462 **occurrence when induced by developmental transitions compared to temperatures**

463 In order to test if DMCs induced by temperature (cold or heat) or embryo development (at 23°C)
464 during SE maturation can be mitotically transmitted to support an epigenetic memory, each
465 DMC class (temperature-, remaining temperature- and development-DMC) was compared to a
466 similar DMC class obtained at another developmental stage (i.e., E-SE vs. C-SE, C-SE vs. SAM
467 for temperature-DMCs, embryonic vs. post-embryonic phase for development-DMCs).
468 Identical DMCs (i.e., found at the same position) with the same hyper-/hypo-methylation status
469 were then identified (Fig. 5A). In the case of unigenes for example, heat (28 vs. 23°C)-induced
470 CG DMCs in E-SE (54,079) were compared to heat-induced CG DMCs in C-SE (40,068) and
471 the 7,232 identical DMCs were filtered for similar methylation status (both hyper- or hypo-
472 methylation). In this way, we identified 4,749 stable, memorized temperature-DMCs (heat)
473 during embryo maturation (11.9% of memorized DMCs, Fig. 5B). Similarly, we found 46,718
474 identical DMCs comparing CG DMCs induced by embryonic development at 23°C (C-SE vs.
475 E-SE) and CG DMCs induced by post-embryonic development (SAM vs. C-SE). After
476 filtration, we identified 23,155 memorized development-DMCs (50% of memorized DMCs).

477 Overall, the percentage of memorized temperature-DMCs (cold or heat) in unigenes (Fig.
478 5B) and gene models (Fig. S3E) was higher in CG and CHG (10-14%) than CHH context (3-
479 5%) during embryonic development (embryonic cold or heat memory). Levels are lower in
480 CG/CHH contexts after post-embryonic development (2-8%) but similar (1-5%) in CHH

481 context (post-embryonic cold or heat memory). The number of unigenes containing at least 1
482 memorized temperature-DMC is higher (all contexts) for cold (4000-8000) than heat (2000-
483 5000) after both embryonic and post-embryonic development (Fig. 4C). In contrast, the
484 percentage of development-DMCs during the embryonic phase at 23°C (E-SE vs. C-SE) that
485 are memorized at the post-embryonic phase (C-SE vs. SAM, Fig. 5B, S3E) is much higher,
486 reaching up to 45-50%, notably in CG/CHG contexts (post-embryonic developmental
487 memory). Regarding promoters (Fig. 5B), no temperature memory could be detected while the
488 post-embryonic developmental memory accounted for up to 90% of memorized DMCs (in CG).

489 GO enrichment analysis for unigenes containing memorized temperature-DMCs (Fig. 6)
490 revealed 6 major groups of GO terms found in 3 out of 4 situations, i.e., cold/heat embryonic
491 (Fig. 6A) or post-embryonic memory (Fig. 6B): 4 groups related with i) heat ('response to heat',
492 2 times with the highest p-values), ii) UV ('response to UV', 'pigment accumulation in response
493 to UV light'), iii) the stress hormone jasmonic acid ('response to jasmonic acid', 'jasmonic acid
494 biosynthesis'), and iv) β -alanine ('beta-alanine metabolism') as a plant defense compound to
495 withstand various stresses (Parthasarathy et al. 2019), and 2 metabolic groups related to v)
496 'Glycolysis/Gluconeogenesis (once with the highest p-value), and vi) 'starch and sucrose
497 metabolism'.

498

499 **Identification of candidate genes under epigenetic control associated with temperature** 500 **memory from embryonic to post-embryonic development**

501 To identify the most significant candidate genes possibly involved in the establishment of a
502 temperature memory, only those containing at least 5 memorized DMCs at the post-embryonic
503 stage (C-SE to SAM) were selected. Excluding genes with no annotation, retrotransposons and
504 rRNA genes, we identified a list of 10 candidate genes (Table 2). Post-embryonic cold memory
505 genes correspond to a Subtilisin-like protein (cell division and embryo development), a Cystein-
506 rich receptor-like protein (defense response), a Histone H3.1 protein (chromatin and regulation
507 of cellular processes) and two proteins involved in the jasmonic acid (JA) pathway (DAD1-like
508 lipase and Cytochrome P450). Post-embryonic heat memory genes match the same Cystein-
509 rich receptor-like protein (defense response), but also a Heat shock protein (protection against
510 heat stress), an Embryo defective MAPK kinase (embryo development, protein
511 phosphorylation), an Arabinogalactan methylesterase (cell wall biogenesis), an ABC
512 transporter family (developmental processes, adaptation), and an Insulinase family protein
513 (embryo development).

514 **DISCUSSION**

515

516 **The methylome landscape of *Pinus pinaster* somatic embryo and tree**

517 Our SE material (Fig. S2B) showed high CG (65-70%) and CHG (55-60%) methylation levels
518 compared to the CHH context (10-20%). This observation is consistent with gymnosperm data
519 from needles (ca. 75/69/1-2%, respectively) and embryogenic tissue (ca. 65/60/3-4%, *Picea*
520 *abies*, Ausin et al. 2016), shoots (ca. 88/82/2%, *Pinus tabuliformis*, Niu et al. 2022), meristems,
521 and young leaves (ca. 78/76/36%, *Welwitschia mirabilis*, Wan et al. 2021). These values
522 support specific roles of CHG/CHH methylation in conifers (Niederhuth et al. 2016, Ausin et
523 al. 2016, Li et al. 2023).

524 We do not confirm that SE material has abnormal CG and CHG methylation patterns (Ausin
525 et al. 2016), but rather specific ones associated with developmental stages (Fig. S4). Compared
526 to other gymnosperm tissues, gene and promoter methylation appeared to be similarly high for
527 C-SE in CG/CHG contexts (up to 70-75%, Fig. S4) but lower for E-SE and SAM. We confirm
528 the high CHH methylation reported by Ausin et al. (2016), but it could be primarily related to
529 development (Fig. S4) as CHH methylation was much higher in C-SE (up to 10-15% in genes,
530 20-35% in promoters) compared to E-SE and SAM (5-10% in genes, 10-20% in promoters).

531 We found higher CG (70 vs. 65%), similar CHG (ca. 55%) and lower CHH (10 vs. 20%)
532 methylation in genes compared to promoters (Fig. S2B). In *P. abies*, Ausin et al. (2016) reported
533 lower gene methylation in all 3 contexts compared to upstream regions. Our results are more
534 aligned with data reported in *P. tabuliformis* (Li et al. 2023) when considering genes with
535 transposable elements (TE, Niu et al. 2022). In this species, genes without TE insertion had
536 much lower methylation levels than promoters in all 3 contexts. Interestingly, gene models had
537 similar (CHH) or lower CG (60%) and CHG (45%) methylation than promoters in our study
538 (Fig. S2B, S3). The regulatory role of gene and promoter methylation has been widely
539 evidenced in angiosperms but was controversial in gymnosperms (Ausin et al. 2016). However,
540 based on a high-quality genome assembly and annotation in *P. tabuliformis*, DNA methylation
541 has been convincingly shown to be negatively correlated with gene expression (Li et al. 2023),
542 especially when targeting exons and gene regions located downstream transcription end site (in
543 all 3 contexts), but also promoters in a more limited way (only in CG context).

544 **The large developmental remodeling of the embryo methylome and epigenetic memory**

545 Characteristic (epi)genomic changes in gene expression at key SE/ZE development stages have
546 been reported in both angiosperms (Narsai et al. 2017, Ji et al. 2019, Chen et al. 2020) and
547 conifers (Vestman et al. 2011, Trontin et al. 2016a). In maritime pine, de Vega-Bartol et al.
548 (2013) reported large sets of differentially expressed genes between stages with evidence for
549 transcriptional regulation by transcription factors (TFs) and epigenetic control, including DNA
550 methylation, chromatin remodeling and non-coding sRNAs. Accordingly, DNA methylation
551 (Fig. S2A) was high in C-SE (29%) compared to E-SE (15%) or plant SAM (25%) and
552 hierarchical clustering (Fig. S2C) further pointed to a specific C-SE pattern, most notably in
553 CHH/CHG contexts of promoters (Fig. S2C, S3B). Profound methylation rearrangements are
554 suggested with an increase during the E-SE/C-SE transition followed by a decrease from
555 embryonic to post-embryonic phase. Such changes have been reported in conifers with either
556 similar (increased in C-SE from ca. 12 to 15-20%, Gao et al. 2022a) or opposite pattern
557 (decreased in C-SE from ca. 61 to 53%, Teyssier et al. 2014).

558 Our methylome analysis revealed that genes exhibited more variation of DNA methylation than
559 promoters in response to development. While similar in the CHH context (1-5%), SMP sites in
560 development-induced DMC reached 6-11% (CG context) and 7-10% (CHG) in genes (Fig. 3C,
561 S3D) as compared to less than 0.1-1.3% in promoters, respectively (Fig. 3D). This might be
562 due to increased plasticity in gene bodies (where small changes have little effects) compared to
563 promoters. Development-DMCs were found mostly hypo-methylated in genes and even more
564 in promoters, notably for CHH and CHG contexts (Fig. S7, Table 1). Accordingly, we found
565 about 25,000 unigenes (12%) containing embryonic and post-embryonic development-DMCs
566 in all 3 contexts, and 4,000-7,000 promoters (8-14%) in the CHH context but less than 2,000
567 (4%) in the CHG or 200 (0.4%) in the CG context (Fig. 4B). The major finding that significant
568 development-DMCs (Fig. S6C) are mainly hypo-methylated in all 3 contexts and rather
569 prevalent in multiple genes is consistent with large developmental reprogramming during both
570 the embryonic and post-embryonic phase towards active expression of large, selected gene
571 pools (Li et al. 2023).

572 Development-induced DMCs during the embryonic phase can be transmitted to the post-
573 embryonic phase (Fig. 5B, S3E) at a high rate in both genes (25-50%) and promoters (18-90%),
574 especially in CG (50-90%) and CHG contexts (50-60%). Such a development-induced
575 epigenetic memory was retained despite the likely massive epigenetic reprogramming during
576 germination (Narsai et al. 2017, Tao et al. 2017, Markulin et al. 2021). This memory is likely
577 to relate to genes whose level of expression established during embryogenesis is critical at least

578 during the juvenile tree phase. We selected 2,500-8,500 genes and 50-1600 promoters
579 containing at least 5 development-DMCs as a stringent criterion (Table 1, Fig. S8B). Main
580 molecular functions of filtered DMCs for embryonic (Mat. S3) and post-embryonic effects (Fig.
581 S9, Mat. S3) were mostly related to germination and early tree growth, as expected.
582 Temperature and heat stress responses were also revealed in both genes and promoters,
583 emphasizing that development is under strong temperature control for both acclimation and
584 tolerance responses in plants (Zhu et al. 2023).

585

586 **Temperature-induced remodeling of the embryo methylome**

587 Temperature is a critical factor affecting embryogenesis, plant growth, and development. We
588 detected a temperature effect on SE hypocotyl size (Fig. S1A) that has been associated with
589 thermomorphogenesis mechanisms involving major TFs (Perella et al. 2022, Zhu et al. 2023).
590 Similar temperature-induced morphological changes were reported in pine (do Nascimento et
591 al. 2020) and we further expanded the observed alterations to cotyledon number. We confirmed
592 data in maritime and radiata pines (Sales et al. 2022, Moncaleán et al. 2018) showing faster
593 growth (Fig. 2E) and/or differences in physiology (Fig. 2D) of somatic seedlings after SE
594 maturation at 23°C compared to 18°C or 28°C. Temperature memory effects on early plant
595 growth were also reported in *P. abies* (Kvaalen and Johnsen 2008) but, as in maritime pine (Fig.
596 S1E), they did not appear to last for long (2 years) unlike phenological traits (at least 6 years,
597 Skrøppa 2022). Both stability and instability of stress memory for different traits could be
598 consistent with an epigenetic determinism.

599 We did not detect global changes in DNA methylation levels (Fig. S2A, 3C) in response to
600 maturation temperature as reported in radiata pine (do Nascimento et al. 2022). In this species,
601 significant variations were found in somatic seedlings by Castander-Olarieta et al. (2020), but
602 following flash temperature treatments at the SE initiation step. Temperature effect could be
603 more pronounced when applied at the early stages of somatic embryogenesis. However, no
604 differences could be observed by Pereira et al. (2021) in Aleppo pine with a similar
605 experimental design.

606 Despite a fairly stable global DNA methylation, we identified thousands of unigenes (ca.
607 25,000, 12%) in E-SE, C-SE, and SAM containing temperature-induced DMCs in all 3
608 methylation contexts (Fig. 4A). Both cold and heat stresses induced similar intensive responses
609 in genes. In contrast, DMCs were found in less than 200 promoters (0.4%). In plants, gene
610 methylation could be a key determinant of environmental stress response regardless of
611 regulatory signals located in the promoter region such as TF binding sites (Aceituno et al. 2008).

612 Regulation of gene expression could be restrained by DNA methylation, especially when
613 occurring in gene exons as shown in pine (Li et al. 2023).

614 As for developmental effects, both genes and promoters containing temperature-induced
615 DMCs showed an enrichment of molecular functions related to metabolisms and response to
616 temperature stress (Fig. S9, Mat. S3). Similarly, we identified mainly in genes molecular
617 functions associated with embryonic development and post-embryonic growth. Temperature
618 sensing could involve a defense response through the jasmonic acid pathway as several related
619 molecular functions have been identified in genes for both cold and heat stress.

620

621 **Epigenetic memory of temperature sensed during embryo maturation in 2-year-old** 622 **regenerated somatic plants**

623 Temperature-induced DMCs can be transmitted from embryonic to post-embryonic phases but,
624 in contrast to development-induced DMCs, at a quite low rate (1-14% vs. 18-90%) and only in
625 genes (Fig. 5B, S3E). We conclude that DNA methylation of the gene rather than the promoter
626 may contribute to the establishment of an epigenetic memory of maturation temperature in
627 maritime pine because it might be more permissive and less tightly controlled. Promoter
628 methylation may be more related to a primary response to temperature involving transient TF
629 binding rather than heat stress memory, which would require more persistent binding (Zhu et
630 al. 2023). Our results are in line with transcriptional profiling of epigenetic regulators during
631 SE development in Norway spruce (Yakovlev et al. 2016) showing that most genes involved in
632 DNA (de)methylation are differentially expressed according to temperature and therefore
633 predicted to be involved in the formation of an epigenetic memory. We significantly expanded
634 upon this finding by demonstrating not only that methylation patterns are established in
635 response to temperature during embryogenesis, but also that they are partially retained in the
636 plant SAM. Temperature-DMCs are memorized at a lower frequency and preferentially in
637 genes compared to development-DMCs, suggesting that DNA methylation contributes to
638 temperature stress memory formation by targeting a different subset of genes and/or genes that
639 are not essential for proper embryo and seedling development. The later hypothesis is supported
640 by our data showing no temperature effect on SE viability and germination rates (Fig. S1C).
641 Yakovlev et al. (2016) discussed that genes involved in embryo development could be weakly
642 responsive to temperature. However, we found good support for molecular functions related to
643 thermosensing of both genes and promoters containing development-DMCs (Fig. S9, Mat. S3).
644 Differential responses to temperature of genes involved in embryogenesis and plant
645 development could partly explain why more memorized temperature-DMCs were observed at

646 the embryonic phase (3-14%) compared to the post-embryonic phase (1-8%) in some contexts
647 (CG, CHG).

648 We found more genes with memorized temperature-DMCs for cold (4000-8000) than for
649 heat (2000-5000) (Fig. 4C). Compared to the reference temperature, cold therefore was a
650 stronger stimulus than heat, emphasizing also that the response could be non-linear. Significant
651 phenotypic variations were indeed observed after maturation at 18°C (Fig. 2, S1) in E-SE
652 (reduced proliferation and glucose content, increased starch content), C-SE (delayed
653 development, reduced yield, fresh mass, hypocotyl size, cotyledons number, and starch
654 content), and plant (chlorosis, reduced growth). Maturation at 28°C had comparatively lower
655 effects.

656 Molecular functions associated with genes containing memorized temperature-induced
657 DMCs (Fig. 6) include defense mechanisms (response to heat, UV, or JA, β -alanine
658 metabolism) and carbon metabolisms (glycolysis, gluconeogenesis, starch and sucrose). In
659 accordance with phenotypic data (Fig. 2, Fig. S1), they were more consistently observed for
660 cold stress. This result emphasized DNA (de)methylation as a regulator of the expression of
661 genes involved in the JA pathway for sensing temperature, not only as a primary perception,
662 but also for stress memory establishment. JA signaling has important roles in plant
663 thermomorphogenesis (Clarke et al. 2009, de Ollas et al. 2015, Khan et al. 2022, Agrawal et al.
664 2022) as well as in embryo and plant development (Elhiti et al. 2013, Wang et al. 2018). It
665 operates through a complex crosstalk with other phytohormone signaling pathways (Maury et
666 al. 2019), especially salicylic acid, ABA, ethylene (stress) and auxin (development). Activation
667 of the JA pathway could be coordinated with regulatory networks such as epigenetic-induced
668 response to heat (Zhu et al. 2023), production of β -alanine as a generic stress response
669 (Parthasarathy et al. 2019), and modulation of primary carbon and carbohydrate metabolisms
670 as key regulators of embryo development (Trontin et al. 2016a) contributing to heat-stress
671 memory (Olas et al. 2021). Accordingly, we found temperature-related changes in glucose,
672 sucrose and starch in both E-SE and C-SE (Fig. S1B).

673 Ten robust candidate genes for epigenetic temperature sensing and memory formation in
674 maritime pine were identified (Table 2). In good concordance with the GO enrichment analyses
675 (Fig. 6, Fig. S9, Mat. S3), they mostly encode proteins involved in defense responses and
676 adaptation and/or embryo development, and also chromatin regulation (see Table 2 for putative
677 role of each gene). Hyper- or hypo-methylation of *Cystein-rich receptor-like protein kinase*
678 gene (*CRK8*) could support both cold and heat memory. Hyper-methylation of *Heat shock*
679 *protein* gene (*HSP*) and hypo-methylation of *ABC transporter family* gene were related with

680 heat stress memory. The JA pathway role in cold stress memory is emphasized by hypo-
681 methylation of *DAD1-like lipase 4* and *Cytochrome P450 (CYP94B3)*. Regarding development-
682 related genes, cold stress memory is supported by hypo-methylation of one *Subtilisin-like*
683 *kinase* gene (*SBT1.8*). Heat stress memory involves hypo-methylation of *Embryo defective 71*
684 *kinase (EMB71)* and *Arabinogalactan methylesterase* genes, and hyper-methylation of
685 *Insulinase family protein M16* gene. Interestingly, cold stress memory was also supported by
686 hypo-methylation of the histone *H3.1* gene involved in the regulation of cellular processes
687 through chromatin rearrangement.

688

689 **Epigenetic control of temperature memory in trees: prospects**

690 DNA methylation (5mC) is currently the epigenetic modification, which can most easily be
691 monitored at both gene and genome levels during memory formation. In the context of climate
692 change, the possibility for early temperature priming during embryogenesis to stimulate plant
693 phenotypic plasticity (e.g., increased tolerance to drought and heat stress) through epigenetic
694 stress memory has great potential in plants, especially in trees with long life cycle and delayed
695 reproductive maturity (Liu et al. 2021, 2022, Sterck et al. 2022, Zhu et al. 2023). If
696 transgenerational stress memory currently appears to be out of reach for trees in an acceptable
697 time frame, intergenerational stress memory can be considered for (epi)genetic breeding
698 applications, including in conifers (Liu and He 2020). Somatic embryogenesis is primarily a
699 promising way to multiply zygotic embryos in a context of seed shortage. Our results and others
700 in conifers (Kvaalen and Johnsen 2008, Moncaleán et al. 2018, Arrillaga et al. 2019, do
701 Nascimento et al. 2020, Sales et al. 2022) showed that temperature variation during early
702 embryogenesis can affect both SE yield and quality and is therefore a way of refining the
703 process towards production of vigorous seedlings of forestry standard, a current limitation of
704 somatic embryogenesis in maritime pine and other conifers (Trontin et al. 2016b, Lelu-Walter
705 et al. 2016). DNA methylation marks associated with optimal SE development as a function of
706 environmental conditions from initiation to maturation (temperature and other abiotic factors:
707 water availability, hormonal balance, nutrition, etc.) could provide new tools for easy
708 monitoring of embryogenic cultures and embryo quality. As a key clonal process to access
709 various technologies in conifers (e.g., cryopreservation, genomic selection, genetic engineering,
710 Klimaszewska et al. 2016), somatic embryogenesis further provides a convenient tool for early
711 priming with abiotic stress in controlled conditions. Our data suggest that temperature-induced
712 memory can be used to modulate early growth of somatic seedlings. Even if temporary, this
713 effect can have important applications in forestry because initial seedling vigor is recognized

714 as a crucial factor for competing with weeds during the first growing season in the field,
715 especially in maritime pine (Trontin et al. 2016b). Interestingly, temperature memory of
716 somatic seedlings can apparently be used to modulate various traits of high interest for
717 plantation forestry in conifers such as plant developmental phenology, tolerance to heat and
718 drought stress (Kvaalen and Johnsen 2008, Castander-Olarieta et al. 2020, Pérez-Oliver et al.
719 2021, 2023, do Nascimento et al. 2022, Sales et al. 2022). Here again, DNA methylation marks
720 could be useful (in conjunction with genetic markers) for managing the production of well-
721 adapted (epi)genetic resources.

722

723 **Acknowledgments**

724 M.D.S. received PhD grants from the French Ministry of Higher Education and Research
725 (MESR). This work was supported by the Centre-Val de Loire Region (France) through the
726 INTEMPERIES project (grant n°2014 00094511 to INRAE, Coord. M.A.L.W.). Scientific and
727 technical support was provided by the epigenomic environmental platform (P2E) of IHPE
728 (<http://ihpe.univ-perp.fr/plateforme-epigenetique/>, Perpignan, France) and by the shared
729 FCBA-INRAE XYLOBIOTECH platform (grant n°ANR-10- EQPX-16, Cestas, Orléans,
730 France), a service from the IN-SYLVA France Research Infrastructure ([https://in-sylva-
731 france.hub.inrae.fr/services/in-lab](https://in-sylva-france.hub.inrae.fr/services/in-lab)). This work was also supported by a grant overseen by the
732 French National Research Agency (ANR) as part of the "Investissements d'Avenir" program
733 (ANR-11-LABX-0002-01, Lab of Excellence ARBRE).

734

735 **Author contributions**

736 S.M. coordinated the research. The plant experimental design was established by J.F.T,
737 M.A.L.W. and S.M. Somatic embryo culture and measurements were performed by I.R. and
738 J.F.T. Somatic plant growth and phenotypic assessments were performed by F.C. and J.F.T.
739 Biochemical analyses were performed by N.B., C.L.M., and C.T. Statistics were performed by
740 J.F.T. (biological data), C.T. (biochemical data), and S.M. (DNA methylation data). DNA
741 extractions and capture were done by A.D. and M.D.S. under ROCHE supervision. HPLC
742 analysis was performed by A.D., M.D.S., and S.M. Sequencing was performed by J.T. and C.D.
743 Design was prepared by A.G. and S.M. Methylome data analysis was done by S.M. and C.C.
744 Gene Ontology analysis was performed by I.M. and S.M. The draft manuscript was conceived
745 and written by J.F.T, C.M., and S.M., and further revised by M.A.L.W. and C.M. All authors
746 approved the final version of the manuscript.

747

748 **ORCID**

749 Jean-François Trontin: <http://orcid.org/0000-0003-4200-2920>

750 Mamadou D. Sow: <https://orcid.org/0000-0002-2815-4939>

751 Alain Delaunay: <https://orcid.org/0000-0002-2519-5380>

752 Inês Modesto: <https://orcid.org/0000-0002-0444-8561>

753 Caroline Teyssier: <https://orcid.org/0000-0001-7106-5483>

754 Isabelle Reymond: No ORCID

755 Francis Canlet: No ORCID

756 Nathalie Boizot: <https://orcid.org/0000-0002-4884-6342>

757 Claire Le Metté: No ORCID

758 Audrey Gibert: No ORCID

759 Cristian Chaparro: <https://orcid.org/0000-0002-5162-349X>

760 Christian Daviaud: No ORCID

761 Jörg Tost: <https://orcid.org/0000-0002-2683-0817>

762 Celia Miguel: <https://orcid.org/0000-0002-1427-952X>

763 Marie-Anne Lelu-Walter: <https://orcid.org/0000-0003-4518-8767>

764 Stephane Maury: <https://orcid.org/0000-0003-0481-0847>

765

766 **Data availability**

767 The data that support the findings of this study are openly available. The Sequence Capture
768 Bisulfite data have been deposited in NCBI at
769 <https://www.ncbi.nlm.nih.gov/bioproject/PRJNA874210>, SRA: SRR21374316,
770 SRR21374315, SRR21374314, SRR21374313, SRR21374312, SRR21374311, SRR21374310,
771 SRR21374309, SRR21374317. Phenotypic data can be found in Mat. S1. Information about the
772 sequence capture design (Roche) and all data from the Metascope analysis are shown in Mat.
773 S2 and S3, respectively, and are available on *data.gouv.fr*, the open platform for French public
774 data (doi: 10.57745/PNGW7G).

775 **REFERENCES**

- 776 Aceituno FF, Moseyko N, Rhee SY, Gutiérrez RA (2008) The rules of gene expression in plants: organ identity
777 and gene body methylation are key factors for regulation of gene expression in *Arabidopsis thaliana*. *BMC*
778 *Genom* 9: 438. doi: 10.1186/1471-2164-9-438
- 779 Adak S, Mandal N, Mukhopadhyay A, Maity PP, Sen S (2023) Current state and prediction of future global climate
780 change and variability in terms of CO₂ levels and temperature. In: Naorem A, Machiwal D (eds) *Enhancing*
781 *Resilience of Dryland Agriculture Under Changing Climate*. Springer, Singapore. doi: 10.1007/978-981-19-
782 9159-2_2
- 783 Agrawal R, Sharma M, Dwivedi N, Maji S, Thakur P, Junaid A, Fajkus J, Laxmi A, Thakur JK (2022) MEDIATOR
784 SUBUNIT17 integrates jasmonate and auxin signaling pathways to regulate thermomorphogenesis. *Plant Physiol*
785 189: 2259-2280. doi: 10.1093/plphys/kiac220
- 786 Akalin A, Kormaksson M, Li S, Garrett-Bakelman FE, Figueroa ME, Melnik A, Mason CE. (2012) MethylKit: a
787 comprehensive R package for the analysis of genome-wide DNA methylation profiles. *Genome Biol* 13: R87.
788 doi: 10.1186/gb-2012-13-10-r87
- 789 Alakärppä E, Salo HM, Valledor L, Cañal MJ, Häggman H, Vuosku J (2018) Natural variation of DNA
790 methylation and gene expression may determine local adaptations of Scots pine populations. *J Exp Bot* 69: 5293–
791 5305. doi: 10.1093/jxb/ery292
- 792 Arrillaga I, Morcillo M, Zanón I, Lario F, Segura J, Sales E (2019) New approaches to optimize somatic
793 embryogenesis in maritime pine. *Front Plant Sci* 10: 138. doi: 10.3389/fpls.2019.00138
- 794 Aryal B, Laurent C, Geisler M (2015) Learning from each other: ABC transporter regulation by protein
795 phosphorylation in plant and mammalian systems. *Biochem Soc Trans* 43: 966–974. doi: 10.1042/BST20150128
- 796 Ausin I, Feng S, Yu C, Liu W, Kuo HY, Jacobsen EL, Zhai J, Gallego-Bartolome J, Wang L, Egertsdotter U,
797 Street NR, Jacobsen SE, Wanga H (2016) DNA methylome of the 20-gigabase Norway spruce genome. *PNAS*
798 113: E8106-E8113. doi: 10.1073/pnas.1618019113
- 799 Benoit M, Simon L, Desset S, Duc C, Cotterell S, Poulet A, Le Goff S, Tatout C, Probst AV (2018) Replication-
800 coupled histone H3.1 deposition determines nucleosome composition and heterochromatin dynamics during
801 *Arabidopsis* seedling development. *New Phytol* 221: 385-398. doi: 10.1111/nph.15248
- 802 Besnard G, Acheré V, Jeandroz S, Johnsen Ø, Faivre Rampant P, Baumann R, Müller-Starck G, Skrøppa T, Favre
803 J-M (2008) Does maternal environmental condition during reproductive development induce genotypic selection
804 in *Picea abies*? *Ann For Sci* 65: 109. doi: 10.1051/forest:2007081
- 805 Birnbaum KD, Roudier F (2017) Epigenetic memory and cell fate reprogramming in plants. *Regeneration* 4: 15-
806 20. doi: 10.1002/reg2.73
- 807 Boivin T, Davi H (2016) Mission d'expertise sur la raréfaction des fructifications du pin maritime dans les Lands
808 de Gascogne. Ministère de l'Agriculture, de l'Agroalimentaire et de la Forêt. [https://hal.archives-ouvertes.fr/hal-](https://hal.archives-ouvertes.fr/hal-01604210)
809 01604210
- 810 Bonhomme M, Peuch M, Ameglio T, Rageau R, Guilliot A, Decourteix M, Alves G, Sakr S, Lacoïnte A (2010).
811 Carbohydrate uptake from xylem vessels and its distribution among stem tissues and buds in walnut (*Juglans*
812 *regia* L.). *Tree Physiol* 30: 89–102. doi: 10.1093/treephys/tpp103
- 813 Brunoni F, Ljung K, Bellinia C (2019) Control of root meristem establishment in conifers. *Physiol Plant* 165: 81–
814 89. doi: 10.1111/ppl.12783

- 815 Cañas RA, Li Z, Belén Pascual M, Castro-Rodríguez V, Ávila C, Sterck L, Van de Peer Y, Cánovas FM (2017)
816 The gene expression landscape of pine seedling tissues. *Plant J* 91: 1064-1087. doi: 10.1111/tpj.13617
- 817 Castander-Olarieta A, Moncaleán P, Pereira C, Pěňčík A, Petřík I, Pavlović I, Novák O, Strnad M, Goicoa T,
818 Ugarte MD, Montalbán IA (2021) Cytokinins are involved in drought tolerance of *Pinus radiata* plants
819 originating from embryonal masses induced at high temperatures. *Tree Physiol* 41: 912–926. doi:
820 10.1093/treephys/tpaa055
- 821 Castander-Olarieta A, Pereira C, Sales E, Meijón M, Arrillaga I, Cañal MJ, Goicoa T, Ugarte MD, Moncaleán P,
822 Montalbán IA (2020). Induction of radiata pine somatic embryogenesis at high temperatures provokes a long-
823 term decrease in DNA methylation/hydroxymethylation and differential expression of stress-related genes.
824 *Plants* 9: 1762. doi: 10.3390/plants9121762
- 825 Chen X, Xu X, Shen X, Li H, Zhu C, Chen R, Munir N, Zhang Z, Chen Y, Xuhan X, Lin Y, Lai Z (2020) Genome-
826 wide investigation of DNA methylation dynamics reveals a critical role of DNA demethylation during the early
827 somatic embryogenesis of *Dimocarpus longan* Lour. *Tree Physiol* 40:1807-1826. doi: 10.1093/treephys/tpaa097
- 828 Clark JS, Andrus R, Aubry-Kientz M et al (2021) Continent-wide tree fecundity driven by indirect climate effects.
829 *Nat Commun* 12: 1242. doi: 10.1038/s41467-020-20836-3
- 830 Clarke SM, Cristescu SM, Miersch O, Harren FJM, Wasternack C, Mur LAJ (2009) Jasmonates act with salicylic
831 acid to confer basal thermotolerance in *Arabidopsis thaliana*. *New Phytol* 182: 175–187. doi: 10.1111/j.1469-
832 8137.2008.02735.x
- 833 Conde D, Le Gac A-L, Perales M, Dervinis C, Kirst M, Maury S, González-Melendi P, Allona I (2017) Chilling-
834 responsive Demeter-like DNA demethylase mediates in poplar bud break: role of active DNA demethylase in
835 trees' bud break. *Plant Cell Environ* 40: 2236–2249. doi: 10.1111/pce.13019
- 836 de Freitas Guedes FA, Nobres P, Ferreira DCR, Menezes-Silva PE, RibeiroAlves M, Correa RL, DaMatta FM,
837 Alves-Ferreira M (2018) Transcriptional memory contributes to drought tolerance in coffee (*Coffea canephora*)
838 plants. *Env Exp Bot* 147: 220–233. doi: 10.1016/j.envexpbot.2017.12.004
- 839 de Ollas C, Arbona V, Gómez-Cadenas A (2015) Jasmonic acid interacts with abscisic acid to regulate plant
840 responses to water stress conditions. *Plant Signal Behav*, 10: 12. doi: 10.1080/15592324.2015.1078953
- 841 Depuydt T, Vandepoele K (2021) Multi-omics network-based functional annotation of unknown *Arabidopsis*
842 genes. *Plant J* 108: 1193-1212. doi: 10.1111/tpj.15507
- 843 de Vega-Bartol JJ, Simões M, Lorenz WW et al (2013) Transcriptomic analysis highlights epigenetic and
844 transcriptional regulation during zygotic embryo development of *Pinus pinaster*. *BMC Plant Biol* 13: 123. doi:
845 10.1186/1471-2229-13-123
- 846 do Nascimento AMM, Montalbán IA, Llamazares De Miguel D, Goicoa T, Ugarte MD, Moncaleán P (2022) High
847 temperature and water deficit cause epigenetic changes in somatic plants of *Pinus radiata* D. Don. *Plant Cell*
848 *Tiss Organ Cult* 151: 107–121. doi: 10.1007/s11240-022-02336-y
- 849 do Nascimento AMM, Barroso PA, Nascimento NFFd, Goicoa T, Ugarte MD, Montalbán IA, Moncaleán P. (2020)
850 *Pinus* spp. somatic embryo conversion under high temperature: effect on the morphological and physiological
851 characteristics of plantlets. *Forests* 11: 1181. doi: 10.3390/f11111181
- 852 Doyle JJ, Doyle JL (1987) A rapid DNA isolation procedure for small quantities of fresh leaf tissue. *Phytochem*
853 *Bull* 19: 11–15. No doi.

- 854 Dugé de Bernonville T, Daviaud C, Chaparro C, Tost J, Maury S (2022) From methylome to integrative analysis
855 of tissue specificity. In: Courdavault V, Besseau S (eds) *Catharanthus roseus*. Methods in Molecular Biology,
856 vol 2505. Humana, New York, NY. doi: 10.1007/978-1-0716-2349-7_16
- 857 Elhiti M, Stasolla C, Wang A (2013) Molecular regulation of plant somatic embryogenesis. *In Vitro Cell Dev Biol*
858 *Plant* 49: 631–642. doi: 10.1007/s11627-013-9547-3
- 859 Gallie DR, Le H, Tanguay RL, Browning KS (1998) Translation initiation factors are differentially regulated in
860 cereals during development and following heat shock. *Plant J* 14: 715-722. doi: 10.1046/j.1365-
861 313x.1998.00175.x
- 862 Gao Y, Chen X, Cui Y, Zhao H, Zhao R, Liu C, Zhao J, Zhang J, Kong L (2022a) Effects of medium supplements
863 on somatic embryo maturation and DNA methylation in *Pseudotsuga gaussenii* Flous, a species under protection.
864 *Forests* 13:288. doi: 10.3390/f13020288
- 865 Gao Z, Zhou Y, He Y (2022b) Molecular epigenetic mechanisms for memory of temperature stresses in plants. *J*
866 *Genet Genom* 49: 991–1001. doi: 10.1016/j.jgg.2022.07.004
- 867 Gautier F, Label P, Eliášová K, Lepélé J-C, Motyka V, Boizot N, Vondráková S, Malbeck J, Trávníčková A, Le
868 Metté C, Lesage-Descauses M-C, Lomenech A-M, Trontin J-F, Costa G, Lelu-Walter M-A, Teyssier C (2019).
869 Cytological, biochemical and molecular events of the embryogenic state in Douglas-fir (*Pseudotsuga menziesii*
870 [Mirb.]). *Front Plant Sci* 10: 118. doi: 10.3389/fpls.2019.00118
- 871 Genitoni J, Vassaux D, Delaunay A, Citerne S, Portillo Lemus L, Etienne MP, Renault D, Stoeckel S, Barloy D,
872 Maury S (2020). Hypomethylation of the aquatic invasive plant, *Ludwigia grandiflora* subsp. *hexapetala* mimics
873 the adaptive transition into the terrestrial morphotype. *Physiol Plant* 170: 280–298. doi: 10.1111/ppl.13162
- 874 Gupta PK, Durzan DJ (1985). Shoot multiplication from mature trees of Douglas-fir (*Pseudotsuga menziesii*) and
875 sugar pine (*Pinus lambertiana*). *Plant Cell Rep* 4:177–179. doi: 10.1007/BF00269282
- 876 Hammond WM, Williams AP, Abatzoglou JT, Adams HD, Klein T, López R, Sáenz-Romero C, Hartmann H,
877 Breshears DD, Allen CD (2022). Global field observations of tree die-off reveal hotter-drought fingerprint for
878 Earth's forests. *Nat Commun* 13: 1761. doi: 10.1038/s41467-022-29289-2
- 879 Hemenway EA, Gehring M (2023) Epigenetic regulation during plant development and the capacity for epigenetic
880 memory. *Ann Rev Plant Biol* 74:87-109. doi: 10.1146/annurev-arplant-070122-025047
- 881 Hofmeister BT, Denkena J, Colomé-Tatché M (2020) A genome assembly and the somatic genetic and epigenetic
882 mutation rate in a wild long-lived perennial *Populus trichocarpa*. *Genome Biol* 21: 259. doi: 10.1186/s13059-
883 020-02162-5
- 884 Hwang J-U, Song W-Y, Hong D, Ko D, Yamaoka Y, Jang S, Yim S, Lee E, Khare D, Kim K, Palmgren M, Yoon
885 H.S, Martinoia E, Lee Y (2016) Plant ABC transporters enable many unique aspects of a terrestrial plant's
886 lifestyle. *Mol Plant* 9: 338–355. doi: 10.1016/j.molp.2016.02.003
- 887 Jacques C, Salon C, Barnard RL, Vernoud V, Prudent M (2021) Drought stress memory at the plant cycle level: a
888 review. *Plants* 10: 1873. doi: 10.3390/plants10091873
- 889 Ji L, Mathioni SM, Johnson S, Tucker D, Bewick AJ, Kim KD, Daron J, Slotkins RK, Jackson SA, Parrott WA,
890 Meyers BC, Schmitz RJ (2019) Genome-wide reinforcement of DNA methylation occurs during somatic
891 embryogenesis in soybean, *The Plant Cell* 31: 2315–2331. doi: 10.1105/tpc.19.00255

- 892 Johnsen Ø, Fossdal CG, Nagy N, MØlmann J, Dæhlen OG, SkrØppa T (2005) Climatic adaptation in *Picea abies*
893 progenies is affected by the temperature during zygotic embryogenesis and seed maturation. *Plant Cell Environ*
894 28: 1090–1102. doi: 10.1111/j.1365-3040.2005.01356.x
- 895 Joly V, Jacob Y (2023) Mitotic inheritance of genetic and epigenetic information via the histone H3.1 variant.
896 *Curr Opin Plant Biol* 75: 102401. doi: 10.1016/j.pbi.2023.102401
- 897 Khan A, Khan V, Pandey K, Sopory SK, Sanan-Mishra N (2022) Thermo-priming mediated cellular networks for
898 abiotic stress management in plants. *Front Plant Sci* 13: 866409. doi: 10.3389/fpls.2022.866409
- 899 Kitaoka N, Matsubara T, Sato M, Takahashi K, Wakuta S, Kawaide H, Matsui H, Nabeta K, Matsuura H (2011)
900 *Arabidopsis* CYP94B3 encodes jasmonyl-L-isoleucine 12-hydroxylase, a key enzyme in the oxidative
901 catabolism of jasmonate. *Plant Cell Physio* 52: 1757–1765. doi: 10.1093/pcp/pcr110
- 902 Klimaszewska K, Hargreaves C, Lelu-Walter MA, Trontin JF (2016) Advances in conifer somatic embryogenesis
903 since year 2000. In: Germanà MA, Lambardi M (eds) *In vitro embryogenesis in Higher plants, Methods in*
904 *Molecular Biology*, vol. 1359, Humana Press, New York, Chap. 7, pp.131–166. doi:10.1007/978-1-4939-3061-
905 6_7
- 906 Klimaszewska K, Noceda C, Pelletier G, Label P, Rodriguez R, Lelu-Walter MA (2009) Biological
907 characterization of young and aged embryogenic cultures of *Pinus pinaster* (Ait). *In Vitro Cell Dev Biol-Plant*
908 45:20–33. doi: 10.1007/s11627-008-9158-6
- 909 Klimaszewska K, Park YS, Overton C, MacEacheron I, Bonga JM (2001) Optimized somatic embryogenesis in
910 *Pinus strobus* L. *In Vitro Cell Dev Biol Plant* 37: 392–399. doi: 10.1007/s11627-001-0069-z
- 911 Koo AJK, Cook TF, Howea GA (2011) Cytochrome P450 CYP94B3 mediates catabolism and inactivation of the
912 plant hormone jasmonoyl-L-isoleucine. *PNAS* 108: 9298–9303. doi: 10.1073/pnas.1103542108
- 913 Kumar G, Rattan UK, Singh AK (2016) Chilling-mediated DNA methylation changes during dormancy and its
914 release reveal the importance of epigenetic regulation during winter dormancy in apple (*Malus x domestica*
915 Borkh.). *PLoS One* 11:e0149934. doi: 10.1371/journal.pone.0149934
- 916 Kvaalen H, Johnsen Å (2008) Timing of bud set in *Picea abies* is regulated by a memory of temperature during
917 zygotic and somatic embryogenesis. *New Phytol* 177: 49–59. doi: 10.1111/j.1469-8137.2007.02222.x
- 918 Lämke J, Bäurle I (2017) Epigenetic and chromatin-based mechanisms in environmental stress adaptation and
919 stress memory in plants. *Genome Biol* 18: 124. doi: 10.1186/s13059-017-1263-6
- 920 Le Gac AL, Lafon-Placette C, Chauveau D, Segura V, Delaunay A, Fichot R, Marron N, Le Jan I, Berthelot A,
921 Bodineau G, Bastien JC, Brignolas F, Maury S (2018) Winter-dormant shoot apical meristem in poplar trees
922 shows environmental epigenetic memory. *J Exp Bot* 69: 4821–4837. doi: 10.1093/jxb/ery271
- 923 Lelu-Walter MA, Klimaszewska K, Miguel C, Aronen T, Hargreaves C, Teyssier C, Trontin JF (2016) Somatic
924 embryogenesis for more effective breeding and deployment of improved varieties in *Pinus* sp.: bottlenecks and
925 recent advances. In: Loyola-Vargas V.M., Ochoa-Alejo N. (Eds), *Somatic Embryogenesis - Fundamental*
926 *Aspects and Applications*, Springer Cham., ISBN 978-3-319-33704-3. Chap. 19, pp. 319–365. doi: 10.1007/978-
927 3-319-33705-0_19
- 928 Li J, Han F, Yuan T (2023) The methylation landscape of giga-genome and the epigenetic timer of age in Chinese
929 pine. *Nat Commun* 14: 1947. doi: 10.1038/s41467-023-37684-6

- 930 Li L, Ye C, Zhao R, Li X, Liu WZ, Wu F, Yan J, Jiang YQ, Yang B (2015) Mitogen-activated protein kinase
931 kinase kinase (MAPKKK) 4 from rapeseed (*Brassica napus* L.) is a novel member inducing ROS accumulation
932 and cell death. *Biochem Biophys Res Commun* 467: 792-7. doi: 10.1016/j.bbrc.2015.10.063
- 933 Litvay JD, Verma DC, Johnson MA (1985) Influence of loblolly pine (*Pinus taeda* L.) culture medium and its
934 components on growth and somatic embryogenesis of the wild carrot (*Daucus carota* L.). *Plant Cell Rep* 4: 325–
935 328. doi: 10.1007/BF00269890
- 936 Liu J, He Z (2020) Small DNA methylation, big player in plant abiotic stress responses and memory. *Front Plant*
937 *Sci* 11: 595603. doi: 10.3389/fpls.2020.595603
- 938 Liu M, Chang W, Yu M, Fan Y, Shang G, Xu Y, Niu Y, Liu X, Zhu H, Dai L, Tang Z, Zhang K, Liu L, Qu C, Li
939 J, Lu K (2021) Overexpression of DEFECTIVE IN ANTHWER DEHISCENCE 1 increases rapeseed silique length
940 through crosstalk between JA and auxin signaling. *Industrial Crops and Products* 168: 113576. doi:
941 10.1016/j.indcrop.2021.113576
- 942 Llebrés MT, Pascual MB, Debille S, Trontin JF, Harvengt L, Ávila C, Cánovas FM (2018) The role of arginine
943 metabolic pathway during embryogenesis and germination in maritime pine (*Pinus pinaster* Ait.). *Tree Physiol*
944 38: 471–484. doi: 10.1093/treephys/tpx133
- 945 Maeji H, Nishimura T (2018) Chapter two - epigenetic mechanisms in plants. *Adv Bot Res* 88: 21–47. doi:
946 10.1016/bs.abr.2018.09.014
- 947 Markulin L, Škiljaica A, Tokic M, Jagic M, Vuk T, Bauer N and Leljck Levanić D (2021) Taking the wheel – de
948 novo DNA methylation as a driving force of plant embryonic development. *Front Plant Sci* 12: 764999. doi:
949 10.3389/fpls.2021.764999
- 950 Matzke MA, Mosher RA (2014) RNA-directed DNA methylation: an epigenetic pathway of increasing
951 complexity. *Nat Rev Genet* 15: 394–408. doi: 10.1038/nrg3683
- 952 Maury S, Sow MD, Le Gac AL, Genitoni J, Lafon-Placette C, Mozgova I (2019) Phytohormone and chromatin
953 crosstalk: the missing link for developmental plasticity? *Front Plant Sci* 10:395. doi: 10.3389/fpls.2019.00395
- 954 Meng LS, Xu MK, Wan W, Yu F, Li C, Wang JY, Wei ZQ, Lv MJ, Cao XY, Li ZY, Jiang JH (2018) Sucrose
955 signaling regulates anthocyanin biosynthesis through a MAPK cascade in *Arabidopsis thaliana*. *Genetics* 210:
956 607-619. doi: 10.1534/genetics.118.301470
- 957 Miguel CM, Rupps A, Raschke J, Rodrigues AS, Trontin JF (2016) Impact of molecular studies on somatic
958 embryogenesis development for implementation in conifer multi-varietal forestry. In: Park YS, Bonga JM, Moon
959 HK (Eds), *Vegetative Propagation of Forest Trees*, KFRI, Seoul, Korea, ISBN 978-89-8176-064-9. pp. 373–421.
960 [https://www.iufro.org/fileadmin/material/science/divisions/div2/20902/vegetative-propagation-of-forest-](https://www.iufro.org/fileadmin/material/science/divisions/div2/20902/vegetative-propagation-of-forest-trees.pdf)
961 [trees.pdf](https://www.iufro.org/fileadmin/material/science/divisions/div2/20902/vegetative-propagation-of-forest-trees.pdf)
- 962 Moncaleán P, García-Mendiguren O, Novák O, Strnad M, Goicoa T, Ugarte MD, Montalbán IA (2018)
963 Temperature and water availability during maturation affect the cytokinins and auxins profile of Radiata pine
964 somatic embryos. *Front Plant Sci* 9: 1898. doi: 10.3389/fpls.2018.01898
- 965 Morel A, Trontin JF, Corbiveau F, Lomenech AM, Beaufour M, Reymond I, Le Metté C, Ader K, Harvengt L,
966 Cadène M, Label P, Teyssier C, Lelu-Walter, MA (2014a) Cotyledonary somatic embryos of *Pinus pinaster* Ait.
967 most closely resemble fresh, maturing cotyledonary zygotic embryos: biological, carbohydrate and proteomic
968 analyses. *Planta* 240: 1075–1095. doi: 10.1007/s00425-014-2125-z

- 969 Morel A, Teyssier C, Trontin JF, Eliášová K, Pešek B, Beaufour M, Morabito D, Boizot N, Le Metté C, Belal-
970 Bessai L, Reymond I, Harvengt L, Cadène M, Corbineau F, Vágner M, Label P, Lelu-Walter MA (2014b) Early
971 molecular events involved in *Pinus pinaster* Ait. somatic embryo development under reduced water availability:
972 transcriptomic and proteomic analyses. *Physiol Plant* 152: 184–201. doi: 10.1111/ppl.12158
- 973 Narsai R, Gouil Q, Secco D, Srivastava A, Karpievitch YV, Liew LC, Lister R, Lewsey MG, Whelan J (2017)
974 Extensive transcriptomic and epigenomic remodelling occurs during *Arabidopsis thaliana* germination. *Genome*
975 *Biol* 18: 172. doi: 10.1186/s13059-017-1302-3
- 976 Nicotra AB, Atkin OK, Bonser SP, Davidson AM, Finnegan EJ, Mathesius U, Poot P, Purugganan MD, Richards
977 CL, Valladares F, van Kleunen M (2010) Plant phenotypic plasticity in a changing climate. *Trends Plant Sci* 15:
978 684–692. doi: 10.1016/j.tplants.2010.09.008
- 979 Niederhuth CE, Bewick AJ, Ji L, Alabady MS, Kim KD, Li Q, Rohr NA, Rambani A, Burke JM, Udall JA, Egesi
980 C, Schmutz J, Grimwood J, Jackson SA, Springer NM, Schmitz RJ (2016) Widespread natural variation of DNA
981 methylation within angiosperms. *Genome Biol* 17: 194. doi: 10.1186/s13059-016-1059-0
- 982 Niu S, Li J, Bo W, Yang W, Zuccolo A, Giacomello S, Chen X, Han F, Yang J, Song Y, Nie Y, Zhou B, Wang P,
983 Zuo Q, Zhang H, Ma J, Wang J, Wang L, Zhu Q, Zhao H, Liu Z, Zhang X, Liu T, Pei S, Li Z, Hu Y, Yang Y,
984 Li W, Zan Y, Zhou L, Lin J, Yuan T, Li W, Li Y, Wei H, Wu HX (2022) The Chinese pine genome and
985 methylome unveil key features of conifer evolution. *Cell* 185: 204–217. doi: 10.1016/j.cell.2021.12.006
- 986 Olas JJ, Apelt F, Annunziata MG, Jhon S, Richard SI, Gupta S, Kragler F, Balazadeh S, Mueller-Roeber B (2021)
987 Primary carbohydrate metabolism genes participate in heat-stress memory at the shoot apical meristem of
988 *Arabidopsis thaliana*. *Mol Plant* 14: 1508-1524. doi: 10.1016/j.molp.2021.05.024
- 989 Palovaara J, Hallberg H, Stasolla C, Luit B, Hakman I (2010) Expression of a gymnosperm PIN homologous gene
990 correlates with auxin immunolocalization pattern at cotyledon formation and in demarcation of the procambium
991 during *Picea abies* somatic embryo development and in seedling tissues. *Tree Physiol* 30: 479–489. doi:
992 10.1093/treephys/tpp126
- 993 Pandian BA, Sathishraj R, Djanaguiraman M, Prasad PVV, Jugulam M (2020) Role of Cytochrome P450 enzymes
994 in plant stress response. *Antioxidants* 9(5): 454. doi: 10.3390/antiox9050454
- 995 Parthasarathy A, Savka MA, Hudson AO (2019) The synthesis and role of β -alanine in plants. *Front Plant Sci* 10:
996 921. doi: 10.3389/fpls.2019.00921
- 997 Paz-Aviram T, Yahalom A, Chamovitz DA (2008) *Arabidopsis* eIF3e interacts with subunits of the ribosome,
998 Cop9 signalosome and proteasome. *Plant Signal Behav* 3: 409-411. doi: 10.4161/psb.3.6.5434
- 999 Pecinka A, Dinh HQ, Baubec T, Rosa M, Lettner N, Scheid OM (2010) Regulation of repetitive elements is
1000 attenuated by prolonged heat stress in *Arabidopsis*. *Plant Cell* 22: 3118–3129. doi: 10.1105/tpc.110.078493
- 1001 Pereira C, Castander-Olarieta A, Sales E, Montalbán IA, Canhoto J, Moncaleán P (2021). Heat stress in *Pinus*
1002 *halepensis* somatic embryogenesis induction: effect in DNA methylation and differential expression of stress-
1003 related genes. *Plants* 10: 2333. doi: 10.3390/plants10112333
- 1004 Perella G, Bäurle I, van Zanten M (2022) Epigenetic regulation of thermomorphogenesis and heat stress tolerance.
1005 *New Phytol* 234: 1144-1160. doi: 10.1111/nph.17970
- 1006 Pérez-Oliver MA, González-Mas MdC, Renau-Morata B, Arrillaga I, Sales E. (2023) Heat-priming during somatic
1007 embryogenesis increased resilience to drought stress in the generated maritime pine (*Pinus pinaster*) plants. *Int*
1008 *J Mol Sci* 24: 9299. doi: 10.3390/ijms24119299

- 1009 Pérez-Oliver MA, Haro JG, Pavlović I, Novák O, Segura J, Sales E, Arrillaga I (2021) Priming maritime pine
1010 megagametophytes during somatic embryogenesis improved plant adaptation to heat stress. *Plants* 10: 446. doi:
1011 10.3390/plants10030446
- 1012 Platt A, Gugger PF, Pellegrini M, Sork VL (2015) Genome-wide signature of local adaptation linked to variable
1013 CpG methylation in oak populations. *Mol Ecol* 24: 3823–3830. doi: 10.1111/mec.13230
- 1014 Plomion C, Bastien C, Bogeat-Triboulot MB, Bouffier L, Déjardin A, Duplessis S, Fady B, Heuertz M, Le Gac
1015 AL, Le Provost G, Legué V, Lelu-Walter MA, Leplé JC, Maury S, Morel A, Oddou-Muratorio S, Pilate G,
1016 Sanchez L, Scotti I, Scotti-Saintagne C, Segura V, Trontin JF, Vacher C (2016) Forest tree genomics: 10
1017 achievements from the past 10 years and future prospects. *Ann For Sci* 73: 77–103. doi: 10.1007/s13595-015-
1018 0488-3
- 1019 Rajpal VR, Rathore P, Mehta S, Wadhwa N, Yadav P, Berry E, Goel S, Bhat V, Raina SN (2022) Epigenetic
1020 variation: a major player in facilitating plant fitness under changing environmental conditions. *Front Cell Dev*
1021 *Biol* 10: 1020958. doi: 10.3389/fcell.2022.1020958
- 1022 Rautengarten C, Steinhauser D, Büssis D, Stintzi A, Schaller A, Kopka J, Altmann T (2005) Inferring hypotheses
1023 on functional relationships of genes: analysis of the *Arabidopsis thaliana* subtilase gene family. *PLoS Comput*
1024 *Biol* 1: e40. doi: 10.1371/journal.pcbi.0010040
- 1025 Rodrigues AS, Chaves I, Costa BV, Lin YC, Lopes S, Milhinhos A, Van de Peer Y, Miguel CM (2019). Small
1026 RNA profiling in *Pinus pinaster* reveals the transcriptome of developing seeds and highlights differences
1027 between zygotic and somatic embryos. *Sci Rep* 9: 11327. doi: 10.1038/s41598-019-47789-y
- 1028 Rodrigues AS, De Vega JJ, Miguel CM (2018) Comprehensive assembly and analysis of the transcriptome of
1029 maritime pine developing embryos. *BMC Plant Biol* 18: 379. doi: 10.1186/s12870-018-1564-2
- 1030 Sáez-Laguna E, Guevara MA, Díaz L-M, Sánchez-Gómez D, Collada C, Aranda I, Cervera M-T (2014) Epigenetic
1031 variability in the genetically uniform forest tree species *Pinus pinea* L. *PLoS One* 9:e103145. doi:
1032 10.1371/journal.pone.0103145
- 1033 Sales E, Cañizares E, Pereira C, Pérez-Oliver MA, Nebauer SG, Pavlović I, Novák O, Segura J, Arrillaga I. (2022)
1034 Changing temperature conditions during somatic embryo maturation result in *Pinus pinaster* plants with altered
1035 response to heat stress. *Int J Mol Sci* 23: 1318. doi: 10.3390/ijms23031318
- 1036 Sarwar R, Li L, Yu J, Zhang Y, Geng R, Meng Q, Zhu K, Tan X-L (2023) Functional characterization of the
1037 Cystine-Rich-Receptor-like Kinases (CRKs) and their expression response to *Sclerotinia sclerotiorum* and
1038 abiotic stresses in *Brassica napus*. *Int J Mol Sci* 24: 511. doi: 10.3390/ijms24010511
- 1039 Schaller (2004) A cut above the rest: the regulatory function of plant proteases. *Planta* 220: 183–197. doi:
1040 10.1007/s00425-004-1407-2
- 1041 Seoane-Zonjic P, Cañas RA, Bautista R, Gómez-Maldonado J, Arrillaga I, Fernández-Pozo N, Gonzalo Claros M,
1042 Cánovas FM, Ávila C (2016) Establishing gene models from the *Pinus pinaster* genome using gene capture and
1043 BAC sequencing. *BMC Genomics* 17: 148. doi: 10.1186/s12864-016-2490-z
- 1044 Seymour DK, Becker C (2017) The causes and consequences of DNA methylome variation in plants. *Curr Opin*
1045 *Plant Biol* 36: 56-63. doi: 10.1016/j.pbi.2017.01.005
- 1046 Singh A, Panwar R, Mittal P, Hassan MdI, Kumar Singh I (2021) Plant cytochrome P450s: role in stress tolerance
1047 and potential applications for human welfare. *Int J Biol Macromol* 184: 874-886. doi:
1048 10.1016/j.ijbiomac.2021.06.125

- 1049 Skrøppa T (2022) Epigenetic memory effects in Norway spruce: are they present after the age of two years? *Scand*
1050 *J Forest Res* 37: 6–13. doi: 10.1080/02827581.2022.2045349
- 1051 Sow MD, Le Gac AL, Fichot R, Lanciano S, Delaunay A, Le Jan I, Lesage-Descauses MC, Citerne S, Caius J,
1052 Brunaud V, Soubigou-Taconnat L, Cochard H, Segura V, Chaparro C, Grunau C, Daviaud C, Tost J, Brignolas
1053 F, Strauss SH, Mirouze M, Maury S (2021) RNAi suppression of DNA methylation affects the drought stress
1054 response and genome integrity in transgenic poplar. *New Phytol* 232: 80–97. doi: 10.1111/nph.17555
- 1055 Sow MD, Allona I, Ambroise C, Conde D, Fichot R, Gribkova S, Jorge V, Le Provost G, Pâques L, Plomion C,
1056 Salse J, Sanchez-Rodriguez L, Segura V, Tost J, Maury S (2018) Chapter twelve - epigenetics in forest trees:
1057 state of the art and potential implications for breeding and management in a context of climate change. *Adv Bot*
1058 *Res* 88: 387–453. doi: 10.1016/bs.abr.2018.09.003
- 1059 Sterck L, de María N, Cañas RA, de Miguel M, Perdiguero P, Raffin A, Budde KB, López-Hinojosa M, Cantón
1060 FR, Rodrigues AS, Morcillo M, Hurel A, Vélez MD, de la Torre FN, Modesto I, Manjarrez LF, Belén Pascual
1061 M, Alves A, Mendoza-Poudereux I, Callejas Díaz M, Pizarro A, El-Azaz J, Hernández-Escribano L, Guevara
1062 MA, Majada J, Salse J, Grivet D, Bouffier L, Raposo R, De la Torre AR, Zas R, Cabezas JA, Ávila C, Trontin
1063 JF, Sánchez L, Alía R, Arrillaga I, González-Martínez SC, Miguel C, Cánovas FM, Plomion C, Díaz-Sala C,
1064 Cervera MT (2022) Maritime pine genomics in focus. In: De la Torre AR (Ed), *The Pine Genome, Compendium*
1065 *of Plant Genomes*. Springer, Cham., Switzerland. pp. 67–123. doi: 10.1007/978-3-030-93390-6_5
- 1066 Stroud H, Do T, Du J, Zhong X, Feng S, Johnson L, Patel DJ, Jacobsen SE (2014) Non-CG methylation patterns
1067 shape the epigenetic landscape in Arabidopsis. *Nat Struct Mol Biol* 21: 64–72. doi: 10.1038/nsmb.2735
- 1068 Tan JW (2023) Molecular analysis of epigenetic memory of stress establishment and long-term maintenance in a
1069 perennial woody plant. Theses and Dissertations, Plant and Soil Sciences, University of Kentucky, USA.
1070 https://uknowledge.uky.edu/pss_etds/166
- 1071 Tao Z, Shen L, Gu X (2017) Embryonic epigenetic reprogramming by a pioneer transcription factor in plants.
1072 *Nature* 551: 124–128. doi: 10.1038/nature24300
- 1073 Temple H, Mortimer JC, Tryfona T, Yu X, Lopez-Hernandez F, Sorieul M, Anders N, Dupree P (2019) Two
1074 members of the DUF579 family are responsible for arabinogalactan methylation in Arabidopsis. *Plant Direct* 3:
1075 e00117. doi: 10.1002/pld3.1117
- 1076 Teyssier C, Maury S, Beaufour M, Grondin C, Delaunay A, Le Metté C, Ader K, Cadene M, Label P, Lelu-Walter
1077 M-A (2014) In search of markers for somatic embryo maturation in hybrid larch (*Larix × eurolepis*): global
1078 DNA methylation and proteomic analyses. *Physiol Plant* 150: 271–291. doi: 10.1111/ppl.12081
- 1079 Trontin J-F, J Raschke, A Rupps (2021) Tree “memory”: new insights on temperature-induced priming effects
1080 during early embryogenesis. *Tree Physiol* 41: 906–911. doi: 10.1093/treephys/tpaa150.
- 1081 Trontin J-F, Klimaszewska K, Morel A, Hargreaves C, Lelu-Walter MA (2016a) Molecular aspects of conifer
1082 zygotic and somatic embryo development: a review of genome-wide approaches and recent insights. In: Germanà
1083 MA, Lambardi M (eds), *In vitro embryogenesis in Higher plants, Methods in Molecular Biology*, vol. 1359,
1084 Humana Press, New York, Chap. 8, pp. 167–207. doi:10.1007/978-1-4939-3061-6_8
- 1085 Trontin JF, Teyssier C, Morel A, Harvengt L, Lelu-Walter MA (2016b) Prospects for new variety deployment
1086 through somatic embryogenesis in maritime pine. In: Park YS, Bonga JM, Moon HK (eds), *Vegetative*
1087 *Propagation of Forest Trees*. National Institute of Forest Science (NIFoS). Seoul, Korea, pp 572–606. ISBN 978-

- 1088 89-8176-064-9. <https://www.iufro.org/fileadmin/material/science/divisions/div2/20902/vegetative-propagation->
1089 [of-forest-trees.pdf](https://www.iufro.org/fileadmin/material/science/divisions/div2/20902/vegetative-propagation-of-forest-trees.pdf).
- 1090 Trösch R, Jarvis P (2011) The stromal processing peptidase of chloroplasts is essential in Arabidopsis, with
1091 knockout mutations causing embryo arrest after the 16-cell stage. *PLoS One* 6(8): e23039. doi:
1092 10.1371/journal.pone.0023039
- 1093 Vestman D, Larsson E, Uddenberg D, Cairney J, Clapham D, Sundberg E, von Arnold S (2011) Important
1094 processes during differentiation and early development of somatic embryos of Norway spruce as revealed by
1095 changes in global gene expression. *Tree Genet Genomes* 7: 347–362. doi: 10.1007/s11295-010-0336-4
- 1096 Vigneaud J, Kohler A, Dia Sow M, Delaunay A, Fauchery L, Guinet F, Daviaud C, Barry KW, Keymanesh K,
1097 Johnson J, Singan V, Grigoriev I, Fichot R, Conde D, Perales M, Tost J, Martin FM, Allona I, Strauss SH,
1098 Veneault-Fourrey C, Maury S (2023) DNA hypomethylation of the host tree impairs interaction with mutualistic
1099 ectomycorrhizal fungus. *New Phytol* 238: 2561-2577. doi: 10.1111/nph.18734
- 1100 von Arnold S, Larsson E, Moschou PN, Zhu T, Uddenberg D, Bozhkov PV (2016) Norway spruce as a model for
1101 studying regulation of somatic embryo development in conifers. In: Park YS, Bonga JM, Moon HK (eds),
1102 *Vegetative Propagation of Forest Trees*. National Institute of Forest Science (NIFoS). Seoul, Korea, pp 351–372.
1103 ISBN 978-89-8176-064-9. [https://www.iufro.org/fileadmin/material/science/divisions/div2/20902/](https://www.iufro.org/fileadmin/material/science/divisions/div2/20902/vegetative-propagation-of-forest-trees.pdf)
1104 [vegetative-propagation-of-forest-trees.pdf](https://www.iufro.org/fileadmin/material/science/divisions/div2/20902/vegetative-propagation-of-forest-trees.pdf)
- 1105 Wan T, Liu Z, Leitch IJ, Xin H, Maggs-Kölling G, Gong Y, Li Z, Marais E, Liao Y, Dai C, Liu F, Wu Q, Song C,
1106 Zhou Y, Huang W, Jiang K, Wang Q, Yang Y, Zhong Z, Yang M, Yan X, Hu G, Hou C, Su Y, Feng S, Yang J,
1107 Chu J, Chen F, Ran J, Wang X, Van de Peer Y, Leitch RL, Wang Q (2021) The *Welwitschia* genome reveals a
1108 unique biology underpinning extreme longevity in deserts. *Nat Commun* 12: 4247. doi: 10.1038/s41467-021-
1109 24528-4.
- 1110 Wang C, Huang J, Li Y, Zhang J, He C, Li T, Jiang D, Dong A, Ma H, Copenhaver G, Wang Y (2022) DNA
1111 polymerase epsilon binds histone H3.1-H4 and recruits MORC1 to mediate meiotic heterochromatin
1112 condensation. *PNAS* 119: e2213540119. doi: 10.1073/pnas.2213540119
- 1113 Wang K, Guo Q, Froehlich JE, Hersh HL, Zienkiewicz A, Howe GE, Benninga C (2018) Two abscisic acid-
1114 responsive plastid lipase genes involved in jasmonic acid biosynthesis in *Arabidopsis thaliana*. *Plant Cell* 30:
1115 1006–1022. doi: 10.1105/tpc.18.00250
- 1116 Wang L, Li Y, Jin X, Liu L, Dai X, Liu Y, Zhao L, Zheng P, Wang X, Liu Y, Lin D, Qin Y (2020) Floral
1117 transcriptomes reveal gene networks in pineapple floral growth and fruit development. *Commun Biol* 3: 500.
1118 doi: 10.1038/s42003-020-01235-2
- 1119 Wasserstein RL, Lazar NA (2016) The ASA statement on *p*-values: context, process, and purpose. *Am Stat* 70:
1120 129-133. doi: 10.1080/00031305.2016.1154108
- 1121 Wedow JM, Yendrek CR, Mello TR, Creste S, Martinez CA, Ainsworth EA (2019). Metabolite and transcript
1122 profiling of Guinea grass (*Panicum maximum* Jacq) response to elevated [CO₂] and temperature. *Metabolomics*
1123 15: 51. doi: 10.1007/s11306-019-1511-8
- 1124 Wiweger M, Farbos I, Ingouff M, Laghercrantz U, von Arnold S (2003) Expression of *Chia4-Pa* chitinase genes
1125 during somatic and zygotic embryo development in Norway spruce (*Picea abies*): similarities and differences
1126 between gymnosperm and angiosperm class IV chitinases. *J Exp Bot* 54: 2691–2699. doi: 10.1093/jxb/erg299

- 1127 Xiao W, Custard KD, Brown RC, Lemmon BE, Harada JJ, Goldberg RB, Fisher RL (2006) DNA methylation is
1128 critical for Arabidopsis embryogenesis and seed viability. *Plant Cell* 18: 805–814. doi: 10.1105/tpc.105.038836
- 1129 Xue T, Liu L, Zhang X, Li Z, Sheng M, Ge X, Xu W, Su Z (2023) Genome-wide investigation and co-expression
1130 network analysis of SBT family gene in *Gossypium*. *Int J Mol Sci* 24: 5760. doi: 10.3390/ijms24065760
- 1131 Yakovlev IA, Viejo M, Fossdal CG (2020) microRNAs in the formation of epigenetic memory in plants: the case
1132 of Norway spruce embryos. In: Miguel C, Dalmay T, Chaves I (eds) *Plant microRNAs. Concepts and Strategies*
1133 *in Plant Sciences*. Springer, Cham. doi: 10.1007/978-3-030-35772-6_4
- 1134 Yakovlev IA, Fossdal CG (2017) In silico analysis of small RNAs suggest roles for novel and conserved miRNAs
1135 in the formation of epigenetic memory in somatic embryos of Norway spruce. *Front Physiol* 8: 674. doi:
1136 10.3389/fphys.2017.00674
- 1137 Yakovlev IA, Carneros E, Lee Y, Olsen JE, Fossdal CG (2016) Transcriptional profiling of epigenetic regulators
1138 in somatic embryos during temperature induced formation of an epigenetic memory in Norway spruce. *Planta*
1139 243: 1237–1249. doi: 10.1007/s00425-016-2484-8
- 1140 Yakovlev IA, Lee Y, Rotter B, Olsen JE, Skrøppa T, Johnsen Ø, Fossdal CG (2014) Temperature-dependent
1141 differential transcriptomes during formation of an epigenetic memory in Norway spruce embryogenesis. *Tree*
1142 *Genet Genomes* 10: 355–366. doi: 10.1007/s11295-013-0691-z
- 1143 Yakovlev IA, Asante DKA, Fossdal CG, Junttila O, Johnsen Ø (2011). Differential gene expression related to an
1144 epigenetic memory affecting climatic adaptation in Norway spruce. *Plant Sci.* 180:132–139. doi:
1145 10.1016/j.plantsci.2010.07.004
- 1146 Yakovlev IA, Fossdal CG, Johnsen Ø (2010) MicroRNAs, the epigenetic memory and climatic adaptation in
1147 Norway spruce. *New Phytol* 187: 1154–1169. doi: 10.1111/j.1469-8137.2010.03341.x
- 1148 Yang X, Wang L, Yuan D, Lindsey K, Zhang X (2013) Small RNA and degradome sequencing reveal complex
1149 miRNA regulation during cotton somatic embryogenesis. *J Exp Bot* 64: 1521–1536. doi: 10.1093/jxb/ert013
- 1150 Yao N, Schmitz RJ, Johannes F (2021) Epimutations define a fast-ticking molecular clock in plants. *Trends Genet*
1151 37: 699-710. doi: 10.1016/j.tig.2021.04.010
- 1152 Zhang H, Lang Z, Zhu JK (2018) Dynamics and function of DNA methylation in plants. *Nat Rev Mol Cell Biol*
1153 19: 489–506. doi: 10.1038/s41580-018-0016-z
- 1154 Zhou Y, Zhou B, Pache L, Chang M, Khodabakhshi AH, Tanaseichuk O, Benner C, Chanda SK (2019) Metascape
1155 provides a biologist-oriented resource for the analysis of systems-level datasets. *Nat Commun* 10: 1523. doi:
1156 10.1038/s41467-019-09234-6
- 1157 Zhu J, Cao X, Deng X (2023) Epigenetic and transcription factors synergistically promote the high temperature
1158 response in plants. *Trends Biochem Sci* 48: 788-800. doi: 10.1016/j.tibs.2023.06.001
- 1159 Zhu R, Shevchenko O, Ma C, Maury S, Strauss SH (2013) Poplars with a PtDDM1-RNAi transgene have reduced
1160 DNA methylation and show aberrant post-dormancy morphology. *Planta* 237: 1483–1493. doi: 10.1007/s00425-
1161 013-1858-4
- 1162 Zimin AV, Stevens KA, Crepeau MW, Puiu D, Wegrzyn JL, Yorke JA, Langley CH, Neale DB, Salzberg SL
1163 (2017) An improved assembly of the loblolly pine mega-genome using long-read single-molecule sequencing.
1164 *GigaScience*, 6(1): giw016. doi: 10.1093/gigascience/giw016

1165 **Tables**

1166

1167 **Table 1:** Main phenotypic and methylome characteristics of somatic embryos (embryonic phase) and corresponding plants (post-embryonic phase)
 1168 after different temperature treatments (18, 23 and 28°C) during maturation (conversion of early embryos to cotyledonary embryos). Temperature
 1169 effects are presented separately from the development effects studied at the reference temperature (23°C, see Fig. 1A for experimental design).

1170 C-SE: Cotyledonary Somatic Embryos; DMC: Differentially Methylated Cytosine; E-SE: Early Somatic Embryos; GO: Gene Ontology; RFOs:
 1171 Raffinose Family Oligosaccharides; SAM: plant Shoot Apical Meristem; SE: Somatic Embryo; SMP: Single Methylation Polymorphism.

Study scale	Temperature effects (18, 23 or 28°C) (cold: 18 vs. 23°C; heat: 28 vs. 23°C)	Development effects (23°C) (embryonic: E-SE vs. C-SE; post-embryonic: C-SE vs. SAM)
Phenotype (embryo growth, development, quality) Fig. 2, S1 Tables S1, S2	<ul style="list-style-type: none"> ● E-SE proliferation increases with temperature. Fig. 2A. ● Cold and heat delayed C-SE development. Table S1. ● Temperature affects C-SE yield (lower at 18/28°C), fresh mass (increasing from 18 to 28°C), size (smaller hypocotyl length/width at 18°C), and morphology (fewer cotyledons at 18°C). Fig. 2B, 2C, S1A. ● No significant differences in total protein content (Mat. S1). ● Higher starch content in E-SE at 18°C and in C-SE at 23°C. Fig. S1B. ● Glucose concentration increased in E-SE with temperature. Sucrose content is lower at 28°C in C-SE. Fig. S1B. ● Disturbed plant physiology during post-embryonic growth after treatment at 18°C (intense yellowing) and 28°C (moderate). Fig. 2D. ● Lower plant height at 8-15 (18/28°C) and 36 months (18°C) originating in the early stages of post-embryonic growth. Fig. 2E, S1D. ● No effect on C-SE germination and viability, plant survival (age 5 to 15 months), height (65 months), and terminal bud elongation in the field (37-62 months). Fig. S1C, S1E, 2F, Table S2. 	<ul style="list-style-type: none"> ● More proteins in C-SE than E-SE (39 vs. 4 µg/mg f.m., Mat. S1) ● C-SE accumulates more starch than E-SE. Fig. S1B ● C-SE contains more sucrose and RFOs (raffinose, stachyose) but less glucose and fructose than E-SE. Fig. S1B.

1172

1173 **Table 1.** Continued

Study scale	Temperature effects (18, 23 or 28°C) (cold: 18 vs. 23°C; heat: 28 vs. 23°C)	Development effects (23°C) (embryonic: E-SE vs. C-SE; post-embryonic: C-SE vs. SAM)
Global methylome (levels and SMPs) Fig. 3, S2-5	<ul style="list-style-type: none"> No significant differences in global DNA methylation ($p = 0.179$) related to development. Fig. S2A. Hierarchical clustering based on SMP occurrence does not discriminate properly between temperatures (18, 23, 28°C). Fig. S2C, S3B. 	<ul style="list-style-type: none"> Significant differences in global DNA methylation related to development (E-SE < C-SE, $p = 0.014$). Fig. S2A. SMP-based clustering of development stages (E-SE, C-SE, SAM) in CHH > CHG > CG and promoter > gene orders. Fig. S2C, S3B.
Differential methylome (DMCs) Fig. 3, 4, S3, S7-9	<ul style="list-style-type: none"> Genes: SMP prevalence in significant temperature- or remaining temperature-DMCs is higher in CG and CHG (3-11%) than CHH (1-5%) contexts. Fig. 3C, S3D. Promoters: SMP prevalence in significant temperature- or remaining temperature-DMCs is considerably lower than in genes (< 0.1 % in all contexts). Fig. 3D. Temperature-DMCs have similar hyper-/hypo-methylation ratios in all contexts. They are most variable for the CHG context (0.308-7.652) compared to CG (0.474-2.321) and CHH (0.333-1.577), and promoters (0.308-7.652) compared to genes (0.286-1.751). Fig. S7. 12% of unigenes (ca. 25,000 out of 206,574) but less than 0.4% of promoters (< 200 out of 51,749) contain temperature- or remaining temperature-DMCs in each context for E-SE, C-SE and SAM. Fig. 4A. 1,500-3,000 (CG) and 1,700-9,500 (CHG/CHH) unigenes contain at least 5 temperature-DMCs. The highest values (8,000-9,000) are observed for C-SE under cold or heat (CHH). Strikingly, no promoters contain at least 5 temperature-DMCs. Fig. S8A. GO enrichment analysis of unigenes/promoters containing DMCs (≥ 5) highlights functions in primary/secondary metabolisms, response to heat and temperature stimulus, especially in promoters. Fig. S9. 	<ul style="list-style-type: none"> Genes: SMP prevalence in significant development-DMCs is higher in CG and CHG (6-11%) than CHH (2-5%) contexts. Fig. 3C, S3D. Promoters: compared to genes, SMP prevalence in significant development-DMCs is lower in CG (< 0.1%) and CHG (< 1.3%) but similar in CHH (1.3-3.1%) contexts. Fig. 3D. Development-DMCs are mostly hypomethylated in genes (ratios: 0.082-0.929) and promoters (0.003-0.446), notably in CHH/CHG contexts (0.003-0.041). Hypomethylation affects both embryonic (0.014-0.929) and post-embryonic DMCs (0.003-0.724). Fig. S7. 12% of unigenes (ca. 25,000) contain development-DMCs and 8-14% promoters in the CHH context (4,000-7,000), but less than 4% in CHG (< 2,000) and 0.4% (< 200) in CG. Fig. 4B. 2,500-3,000 (CG) to 7,000-8,500 (CHG/CHH) unigenes contain at least 5 development-DMCs with similar figures at the embryonic and post-embryonic phases. This is far fewer promoters and only in CHG (50-60) and CHH (619-1605) contexts. Fig. S8B. GO enrichment analysis of unigenes/promoters containing DMCs (≥ 5) reveals functions in primary/secondary metabolisms and also, intriguingly, response to temperature stimulus. Fig. S9.

1174

1175 **Table 1. End**

Study scale	Temperature effects (18, 23 or 28°C) (cold: 18 vs. 23°C; heat: 28 vs. 23°C)	Development effects (23°C) (embryonic: E-SE vs. C-SE; post-embryonic: C-SE vs. SAM)
Memory methylome (conserved DMCs) Fig. 4-6, S3 Table 2	<ul style="list-style-type: none"> ● Temperature-DMCs can be transmitted from embryonic (E-SE to C-SE) to post-embryonic (C-SE to SAM) phases. Fig. 4C, Fig. 5. ● Genes: levels of temperature-induced memory (% memorized DMCs) during the embryonic phase are higher in CG/CHG (10-14%) than CHH (3-5%) context. Post-embryonic levels are lower in CG/CHG (2-8%) but similar in CHH context (1-5%). Fig. 5B, S3E. ● Promoters: no temperature-induced memory could be detected after both embryonic and post-embryonic development. Fig. 5B. ● There are more genes containing memorized DMCs for cold (4000-8000) than for heat (2000-5000) after both embryonic and post-embryonic development (Fig. 4C). ● GO enrichment analysis of temperature-induced memory in unigenes unravel molecular functions related with stress response (mainly heat, UV, jasmonic acid, beta-alanine metabolism) and carbohydrate metabolisms (glycolysis/gluconeogenesis, starch and sucrose). Fig. 6. ● Annotated genes containing most memorized DMCs (≥ 5) at the post-embryonic phase (CSE to SAM) relate to proteins involved in defense/adaptation responses (cold/heat: Cystein-rich receptor-like; cold: DAD1-like lipase, Cytochrome P450; heat: Heat shock protein, ABC transporter), chromatin regulation (heat: Histone H3.1), and embryo development (cold: Subtilisin-like; heat: Embryo defective MAPK kinase, arabinogalactan methylesterase, insulinase). Table 2. 	<ul style="list-style-type: none"> ● Development-DMCs (identified in C-SE vs. E-SE) can be transmitted to the post-embryonic phase (C-SE to SAM). Fig. 5. ● Genes: levels of development-induced memory (% memorized DMCs) observed after the post-embryonic phase (C-SE to plant SAM at 23°C) reached 45-50% in CG/CHG contexts and 25-42% in CHH context. Fig. 5B, S3E. ● Promoters: compared to genes, levels of development-induced memory are similar in CHH (18%) or higher for CG (90%) and CHG (61%) contexts. Fig. 5B.

1176

1177 **Table 2:** Best-annotated candidate genes for post-embryonic memory of temperature during embryo maturation in *Pinus pinaster*.
 1178 Unigene ID in *Pinus pinaster* (Pp) and best corresponding hits in *Arabidopsis thaliana* (At) and *Pinus taeda* (Pt) are given for candidate genes
 1179 containing at least 5 differentially-methylated cytosines (DMC) with consistent hyper- or hypo-methylation status in a given methylation context
 1180 (CG, CHG, or CHH; H = A, C, or T). DMCs established in C-SE and memorized in the plant SAM in response to heat (28 vs. 23°C) or cold (18
 1181 vs. 23°C).

Memory	Unigene ID (Pp) Best hit (At) Best hit (Pt)	DMC (N) Status Context	Candidate gene annotation and putative role
Heat	isotig48570 AT3G23990 PITA_05635	5 Hyper CHG	Heat shock protein (HSP) HSP acts as a molecular chaperone, assisting in protein folding, recovery of denatured proteins under stress conditions, and also in protein synthesis during cell growth and survival. Both epigenetic primary heat stress responses and formation of heat stress memory contribute to plant thermomorphogenesis under optimal or temperature stress (Zhu et al. 2023). It involves complex, coordinated epigenetic, transcriptional and co-transcriptional regulation in the meristems of heat-shock TFs (HSFs, e.g., HSFA1, A2 and PIF4 as the hub of thermomorphogenetic signaling pathway in plants with homologs in conifers, Yakovlev et al. 2016, Agrawal et al. 2022), heat-induced metabolic enzymes (including primary carbohydrate metabolism, Olas et al. 2021), heat-signaling proteins and HSPs (e.g., HSP17, 20-22, 70, 101). Zhu et al. (2023) highlighted the significant roles of both histone (especially histone H3) and chromatin structure modifications in epigenetic heat stress memory induced by temperature stress involving HSPs. As discussed by these authors, we further provided strong evidence for involvement of DNA methylation in temperature stress memory targeting at least HSPs. Temperature priming during somatic embryogenesis initiation was previously shown to affect HSP gene expression in both maritime (HSP70, Pérez-Oliver et al. 2021) and other pines (Castander-Olarieta et al. 2020, Pereira et al. 2021).
Heat	unigene38126 AT1G54350 PITA_04143	7 Hypo CHH	ABC transporter family protein This family is highly expanded in higher plants and can transport various compounds across membranes such as phytohormones and secondary metabolites involved in developmental processes and adaptation to environmental cues such as dry conditions (Hwang et al. 2016). ABC transporter proteins are directed towards the plasma membrane by interacting with other proteins, including HSPs (Aryal et al. 2015). It is suggested that coordinated (de)methylation of ABC transporter and HSP genes could contribute to thermomorphogenesis driven by heat stress memory.

1182

1183 **Table 2.** Continued

Memory	Unigene ID (Pp) Best hit (At) Best hit (Pt)	DMC (N) Status Context	Candidate gene annotation and putative role
Heat	unigene38171 AT1G63700 PITA_34649	6 Hypo CHH	Embryo defective 71, MAP Kinase Kinase Kinase 4 (EMB71) This protein kinase gene from the large MAPKKK family (<i>Embryo defective 71/EMB71</i> , also named YODA/YDA or MAPKKK4) has been involved in regulatory pathways for embryo and stomatal development, drought tolerance and other stress responses such as accumulation of anthocyanins or reactive oxygen species inducing cell death (Li et al. 2015, Meng et al. 2018). The YDA signaling pathway also regulates early embryo patterning through phosphorylation of a TF gene (<i>WRKY2</i>), which in turn activates <i>WOX8</i> involved in embryo apical-basal polarization (Markulin et al. 2021). Interestingly, mutation in <i>MET1</i> (CG methylation) affects DNA methylation and expression of <i>YDA</i> , <i>WOX8</i> and other genes involved in embryo development (Xiao et al. 2006). Mutations in <i>YDA</i> result in embryo lethality.
Heat	isotig13597 AT1G27930 PITA_48412	5 Hypo CG	Arabinogalactan methyltransferase (AGM) AGMs are involved in glucuronic acid methylation of arabinogalactan proteins (AGPs), a plant cell wall component (Temple et al. 2019). In Arabidopsis, AGM1 interacts with the “e” subunit (eIF3e) of translation initiation factor 3 (eIF3, Paz-Aviram et al. 2008). Most eIF3 factors are known to differentially accumulate from early to late embryo/seed development in plants and, interestingly, following heat shock (Gallie et al. 1998). It is suggested that temperature stress could affect the AGM1/eIF3e interaction and modify the status of AGP methylation. In conifers, AGPs located in the epidermal cell wall are considered as extracellular signal molecules. They could be targeted by specific chitinases that are involved in programmed cell death (PCD), a required process for embryo development (Wiweger et al. 2003). In maritime pine, chitinases were found upregulated at the onset of embryo development (E-SE stage, Morel et al. 2014b).
Heat	unigene38616 AT1G06900 PITA_33033	6 Hyper CHG	Insulinase (peptidase family M16) family protein Insulinase family protein M16 is a stromal processing peptidase (SPP) encoding a chloroplast-localized metalloprotease involved in protein catabolic process with crucial roles in embryo development (Trösch and Jarvis 2011), chloroplast biogenesis and plant survival (Schaller 2004). Interestingly, analyses of down-regulated mutants for <i>SPP</i> in plants showed delayed embryo development and high rate of embryo lethality, reduced number and underdeveloped chloroplasts associated with chlorotic phenotypes (Trösch and Jarvis 2011, and references therein). Hyper-methylation of this insulinase gene (and likely downregulated expression) could explain delayed embryo development at 28°C in our experiment and needle chlorosis of the resulting plants (Fig. 2D). Such mechanisms may also apply for cold stress memory as we observed similar phenotypes.

1184

1185 **Table 2.** Continued

Memory	Unigene ID (Pp) Best hit (At) Best hit (Pt)	DMC (N) Status Context	Candidate gene annotation and putative role
Heat	unigene8836	5 Hyper CHG	Cystein-rich receptor-like protein kinase 8 (CRK8) CRK8 is a transmembrane protein involved in defense response and protein phosphorylation (regulation of stress signaling) as well as development-related pathways (Sarwar et al. 2023). This gene was shown to be the target of specific miRNA during SE development in cotton (Yang et al. 2013) and its expression has been negatively correlated with melibiose accumulation at elevated temperature in plants (Wedow et al. 2019). We found <i>CRK8</i> hyper-methylated under heat stress and hypo- or hyper-methylated under cold stress. The possible resulting variation in gene expression may be associated with soluble carbohydrate content as osmotic regulation under temperature stress. Interestingly <i>CRK8</i> is expressed in guard cells in <i>Panicum maximum</i> suggesting a role in stomatal response (Wedow et al. 2019). Melibiose remained below detection limit in our experiment but we observed changes in other diholosides (sucrose, fructose) in E-SE and C-SE. Changes in membrane fluidity and calcium flux is considered as a primary temperature sensing mechanism in plants that are thought to activate signal transduction events based on Ca ²⁺ -signaling kinases such as CRKs (Yakovlev et al. 2016, Sarwar et al. 2023).
Cold	unigene46117	7 Hypo CHG	
Cold	unigene49512 AT4G23160 PITA_00978	8 Hyper CHG	
Cold	unigene40492 AT2G05920 PITA_20033	6 Hypo CG	Subtilisin-like (SBT1.8), subtilase family protein (protease) SUBTILISIN-LIKE KINASE (subtilases, SBT) belongs to a super-family of serine proteases involved in control of embryonic and post-embryonic development and stress tolerance by regulating cell wall properties, protein turnover and downstream components of signaling cascades (Rautengarten et al. 2005). The SBT1 branch of the family includes several members related to stress (Xue et al. 2023). More specifically, the <i>SBT1.8</i> gene found hypomethylated in our study has been involved in reproductive plant development (Wang et al. 2020) and appeared to be downregulated by abiotic stress in <i>Gossypium</i> (Xue et al. 2023). It has functional relationships in <i>Arabidopsis</i> with <i>Leafy Cotyledon 1 (LEC1)</i> , an important gene in plants for early embryogenesis and the switch between embryonic and post-embryonic development (Depuydt and Vandepoele 2021), including in conifers (Miguel et al. 2016, Trontin et al. 2016a).

1186

1187 **Table 2.** Continued.

Memory	Unigene ID (Pp) Best hit (At) Best hit (Pt)	DMC (N) Status Context	Candidate gene annotation and putative role
Cold	unigene9797 AT5G65360 PITA_32820	5 Hypo CHG	Histone H3 H3.1, histone superfamily protein In Arabidopsis, H3.1 is deposited in nucleosomes specifically during the S phase of DNA replication by the Chromatin Assembly Factor 1 (CAF1). Nucleosome H3.1 enrichment is observed during chromocenter formation (i.e., clustering of repetitive heterochromatic loci) regulating transcriptional repression in both meiotic (Wang et al. 2022) and mitotic heterochromatin (Benoit et al. 2018). Chromocenters contribute to both silencing of transposons and other repetitive elements through genome partitioning and structuring of heterochromatic and euchromatic domains required at specific embryonic or post-embryonic developmental stages (e.g., during early seedling development, Benoit et al. 2018) and response to environmental stimuli such as heat stress (Pecinka et al. 2010). Repetitive sequences are enriched in some repressive chromatin marks such as DNA methylation and post-translational modification of histone H3 variants but their clustering in chromocenters required increased deposition of H3.1 and other histones. Interestingly, behind its role in preventing genome instability, Joly and Jacob (2023) recently put emphasis on the specific role of H3.1 deposition for the mitotic inheritance of both genetic information and epigenetic states. In our study, DNA hypomethylation could have enhanced <i>H3.1</i> gene expression following cold stress during embryo maturation. Increased H3.1 deposition would have in turn promoted the transmission of temperature-induced DMCs in stress- and development-related genes (those discussed above and others) from embryonic to post-embryonic development.
Cold	isotig49597 AT1G51440 PITA_34025	5 Hypo CG	DAD1-like lipase 4, phospholipase A1-Igamma1 Defective in Anther Dehiscence 1 (DAD1) is a plastidial phospholipase A1 that hydrolyzes phosphatidylcholine, glycolipids as well as triacylglycerols. This lipase is mostly expressed in reproductive tissues and seeds and involved in activation of JA biosynthesis genes (Wang et al. 2018). When overexpressing DAD1, JA genes were upregulated in rapeseeds with coordinated down regulation of Auxin response factor 18 involved in reproductive development (Liu et al. 2021). DAD1 has a critical role in the crosstalk between JA and auxin signaling pathways to regulate thermomorphogenesis in plants (Agrawal et al. 2022).

1188

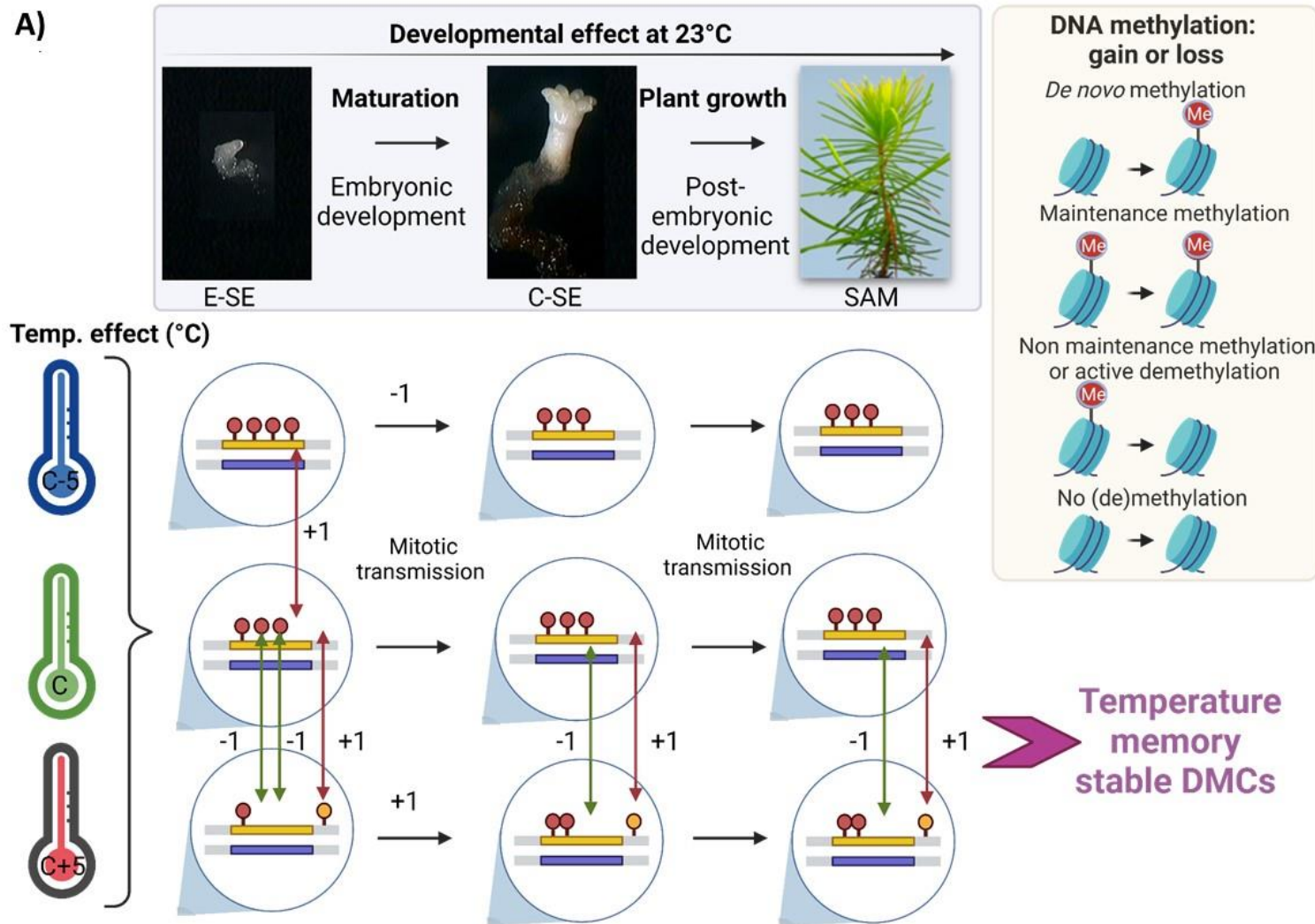
1189 **Table 2.** End.

Memory	Unigene ID (Pp) Best hit (At) Best hit (Pt)	DMC (N) Status Context	Candidate gene annotation and putative role
Cold	isotig24982 AT3G48520 PITA_30677	6 Hypo CG	Cytochrome P450 (CYP94B3) <i>CYP94B3</i> is a member of the Cytochrome P450 monooxygenase family genes CYP94 involved in turnover of jasmonoyl-L-isoleucine hormone (JA-Ile), the receptor-active form of JA (Koo et al. 2011). <i>CYP94B3</i> encodes a jasmonoyl-L-isoleucine 12-hydroxylase mediating catabolism and inactivation of JA-Ile. CYP94B3 transcript levels rise in response to wounding. Fatty acid hydroxylation is involved in cuticle formation and plant signaling with the specific role of CYP94B3 in coordinated JA and SA signaling. Enhanced expression of <i>CYP94B3</i> could attenuate the JA signaling cascade by controlling the JA-Ile levels (Kitaoka et al. 2011). Cytochrome P450 genes are highly expressed during somatic embryogenesis in conifers (Trontin et al. 2016a) and have various roles in growth, development, and stress tolerance, especially through biosynthesis and homeostasis of phytohormones including ABA and JA (Pandian et al. 2020, Singh et al. 2021, Agrawal et al. 2022).

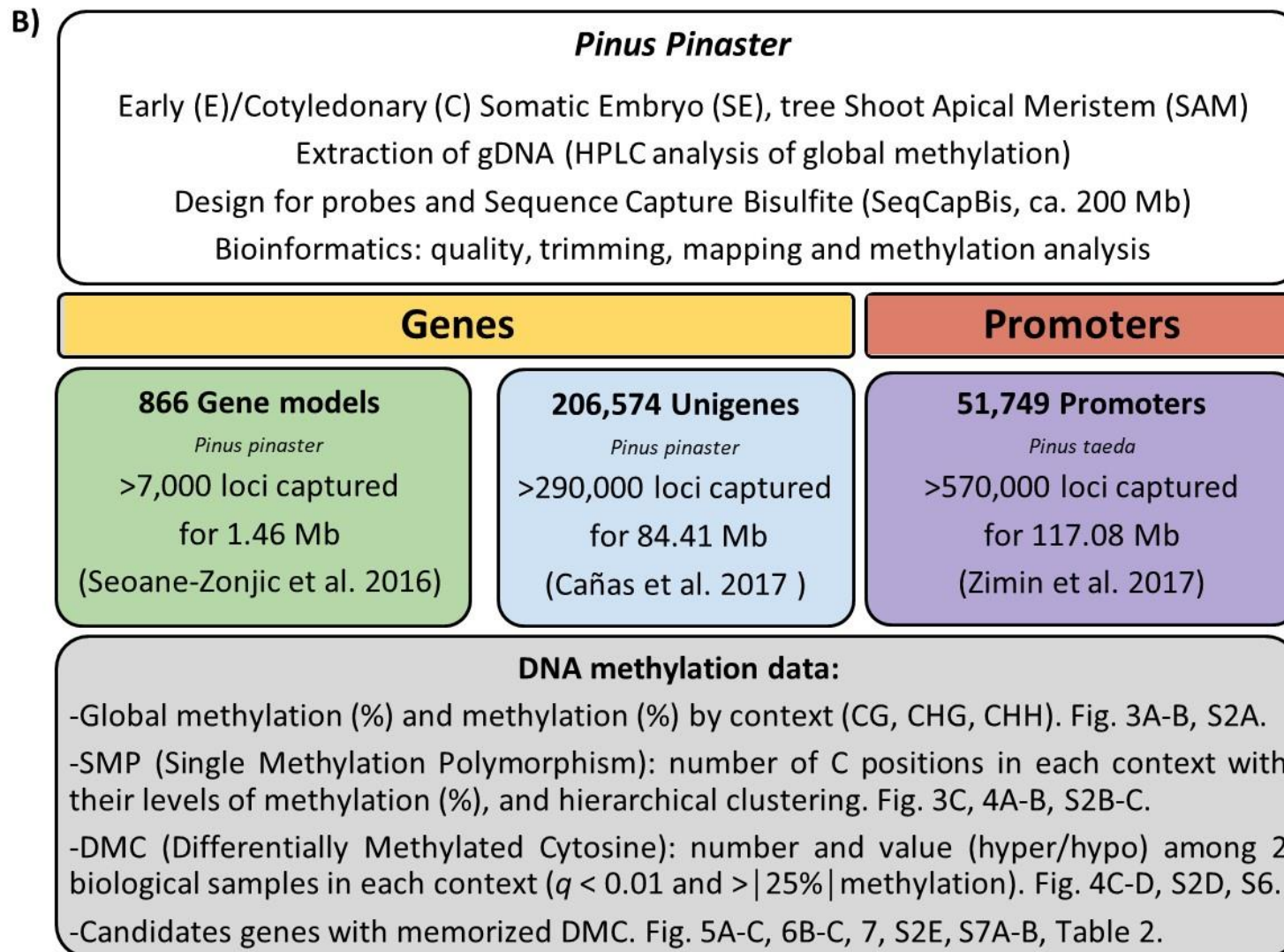
1190

1191 **Figures**

1192



1193

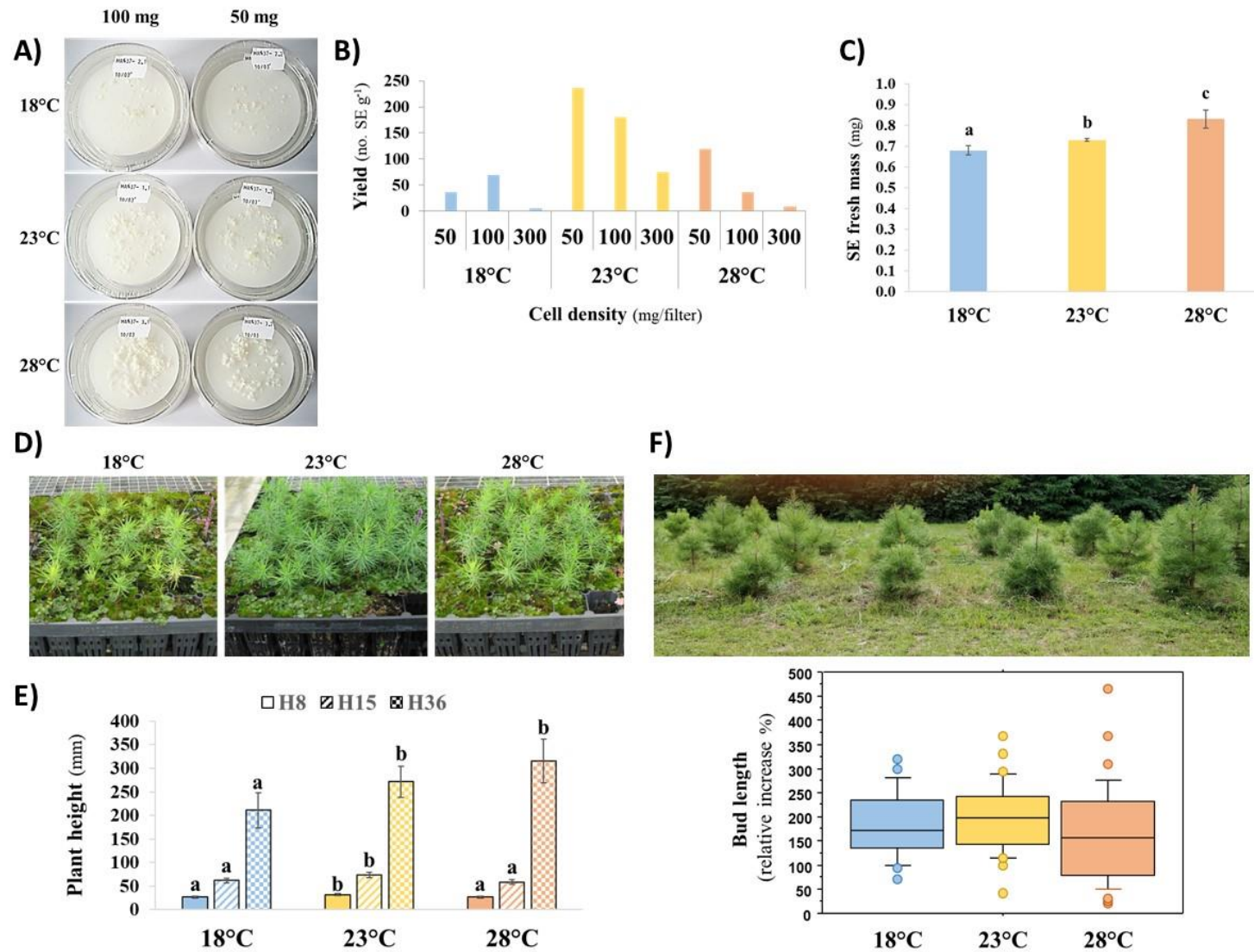


1194

1195 **Figure 1:** Experimental designs for production of biological material (A) and DNA methylation analyses (B).

1196 **A.** The PN519 embryogenic line was reactivated from the cryopreserved stock (2 weeks) and propagated until the embryogenic masses were fully
1197 established (8 additional weeks), i.e., consisting of multiple, actively multiplying immature somatic embryos (SE). This initial step of the embryonic
1198 phase of development (early embryogenesis) was performed at the reference control temperature (C = 23°C). Embryogenic masses were then
1199 subjected to 3 temperature treatments (18, 23 and 28°C, i.e., C-5, C, and C+5) during the whole maturation phase to produce early SE (E-SE, after
1200 1 week) and cotyledonary SE samples (C-SE, after 11-17 more weeks). After storage at 4°C for 4-5 months (embryo post-maturation treatment
1201 and synchronization), the C-SE were germinated at 23°C (3 weeks) and the resulting plantlets were gradually acclimated (4 months; 23-25°C) and
1202 further grown in greenhouse conditions (16 months; 15-30°C) to obtain collectable shoot apical meristems (SAM). At this stage of the post-
1203 embryonic development, somatic plants were 21 months old since germination (juvenile vegetative phase). E-SE, C-SE and plants were phenotyped
1204 at various times around the sampling date for methylome analysis to study temperature effects (cold: 18 vs. 23°C; heat: 28 vs. 23°C) as well as
1205 development effects (at 23°C). This fully clonal design allowed testing for temperature- and/or development-induced memory from embryonic (E-
1206 SE vs. C-SE, heterotrophic state) to post-embryonic phase (C-SE vs. SAM, photosynthetically competent state). For this purpose, DNA methylation
1207 analyses were performed at cytosine sites to identify gain (+1) or loss (-1) in 5 methylcytosine (5mC). Such methylation marks were checked for
1208 mitotic transmission between developmental stages.

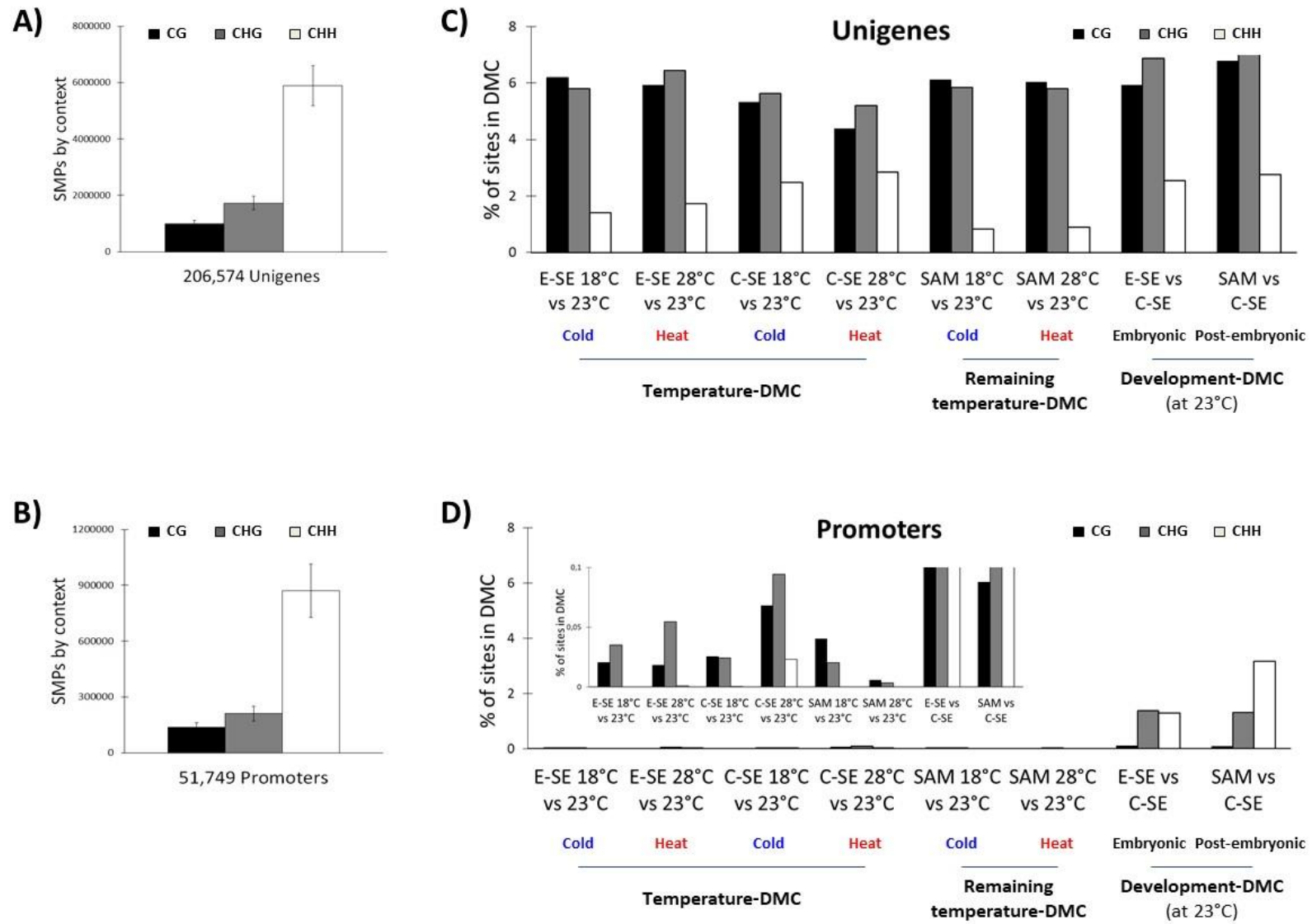
1209 **B.** Genomic DNA (gDNA) was extracted from E-SE, C-SE, and SAM samples for both HPLC (global DNA methylation) and sequence capture
1210 bisulfite (methylome) analyses. After sequence quality control using bioinformatic tools, over 867,000 loci were successfully captured in gene
1211 models (> 7,000 loci), unigenes (> 290,000 loci) and promoters (> 570,000 loci). We analyzed the global DNA methylation level, the percentage
1212 of methylation by context, the occurrence of single methylation polymorphisms (SMPs) and differentially methylated cytosines (DMCs). We
1213 finally identified candidate genes with memorized DMCs at the embryonic or post-embryonic phase.



1214

1215 **Figure 2:** Effect of temperature during maturation (18, 23, 28°C) on embryonic and post embryonic development of PN519 somatic embryos.

- 1216 **A.** Observed embryogenic tissue proliferation after 1 week maturation at 2 cell densities (100 and 50 mg / filter). Note that cell growth increases
1217 with temperature.
- 1218 **B.** Yield in cotyledonary somatic embryos (C-SE) according to initial cell density (50-300 mg/filter) and temperature after 12-13 (23°C), 15-16
1219 (23°C) or 17-18 weeks (18°C) maturation time.
- 1220 **C.** Mean fresh mass of cotyledonary somatic embryos (C-SE). Bars: 95% confidence limits. Significant differences ($p < 0.05$) are indicated by
1221 different letters. The difference observed between 18 or 23°C and 28°C is significant at $p < 0.01$.
- 1222 **D.** Somatic plant behavior 15 months after germination. Note the apparent, general yellowing (chlorosis) of the plant batches from embryos treated
1223 at 18°C and 28°C compared to the standard, greener batch (23°C).
- 1224 **E.** Mean plant height at age 8 (H8), 15 (H15) and 36 months (H36). Growth in the greenhouse (H8, H15) or at field (H36). Bars: 95% confidence
1225 limits. For each variable, significant differences are indicated by different letters at $p < 0.01$ (H8, H15) or 0.05 (H36).
- 1226 **F.** Relative increase in length of plant terminal bud during spring 2019 (age 37-38 months) and 2021 (age 61-62 months). Box plot displaying the
1227 10th, 25th, 50th, 75th, and 90th percentiles and outliers. ANOVA did not detect any significant effect between year and temperature conditions.
1228 Picture: a view of the field trial at age 65 months.

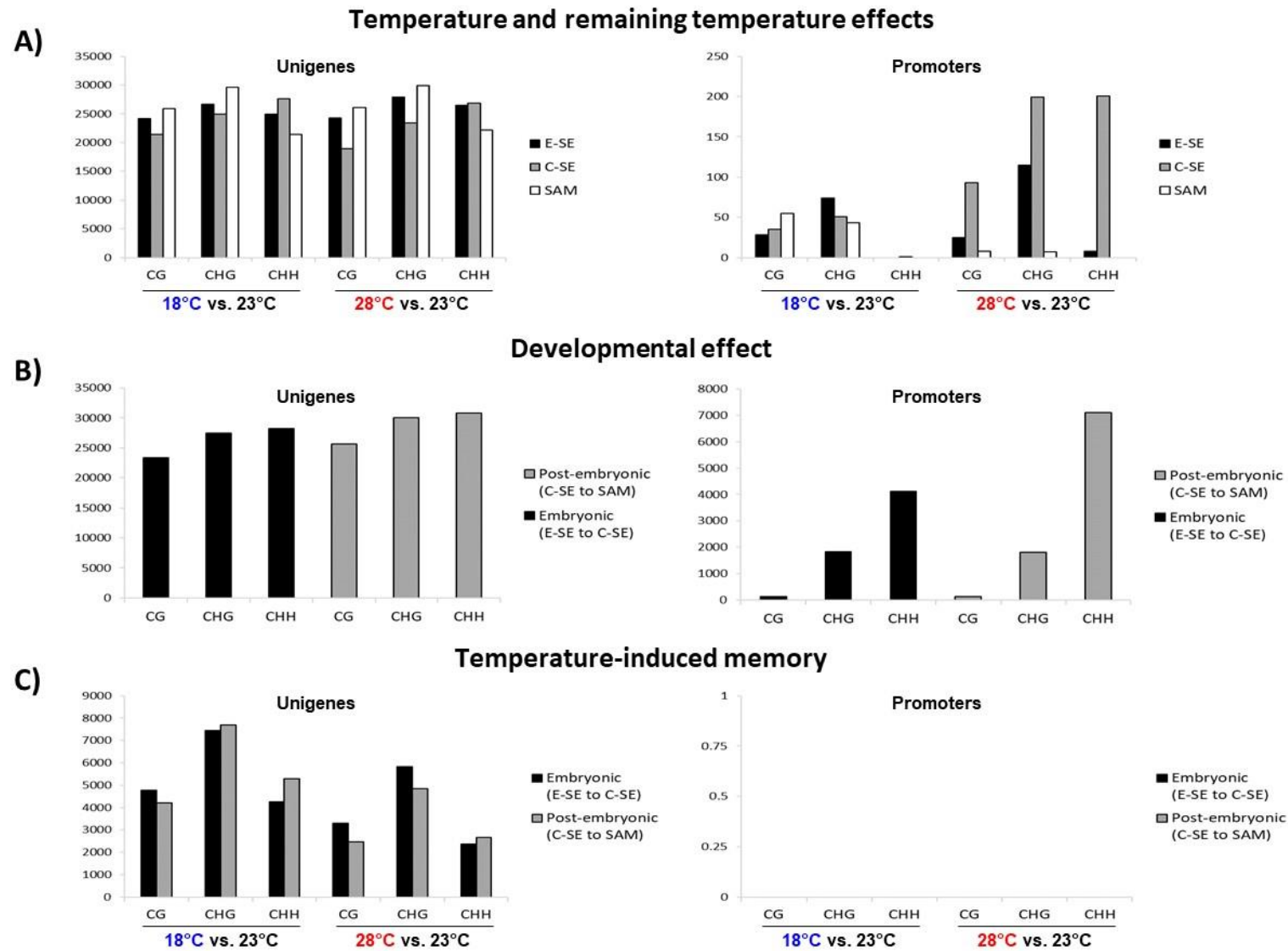


1229

1230 **Figure 3:** Differential Methylation.

1231 **A-B.** Number of Single Methylation Polymorphisms (SMPs) detected in the 3 contexts of methylation (CG, CHG, CHH). **A.** Unigenes; **B.**
1232 Promoters.

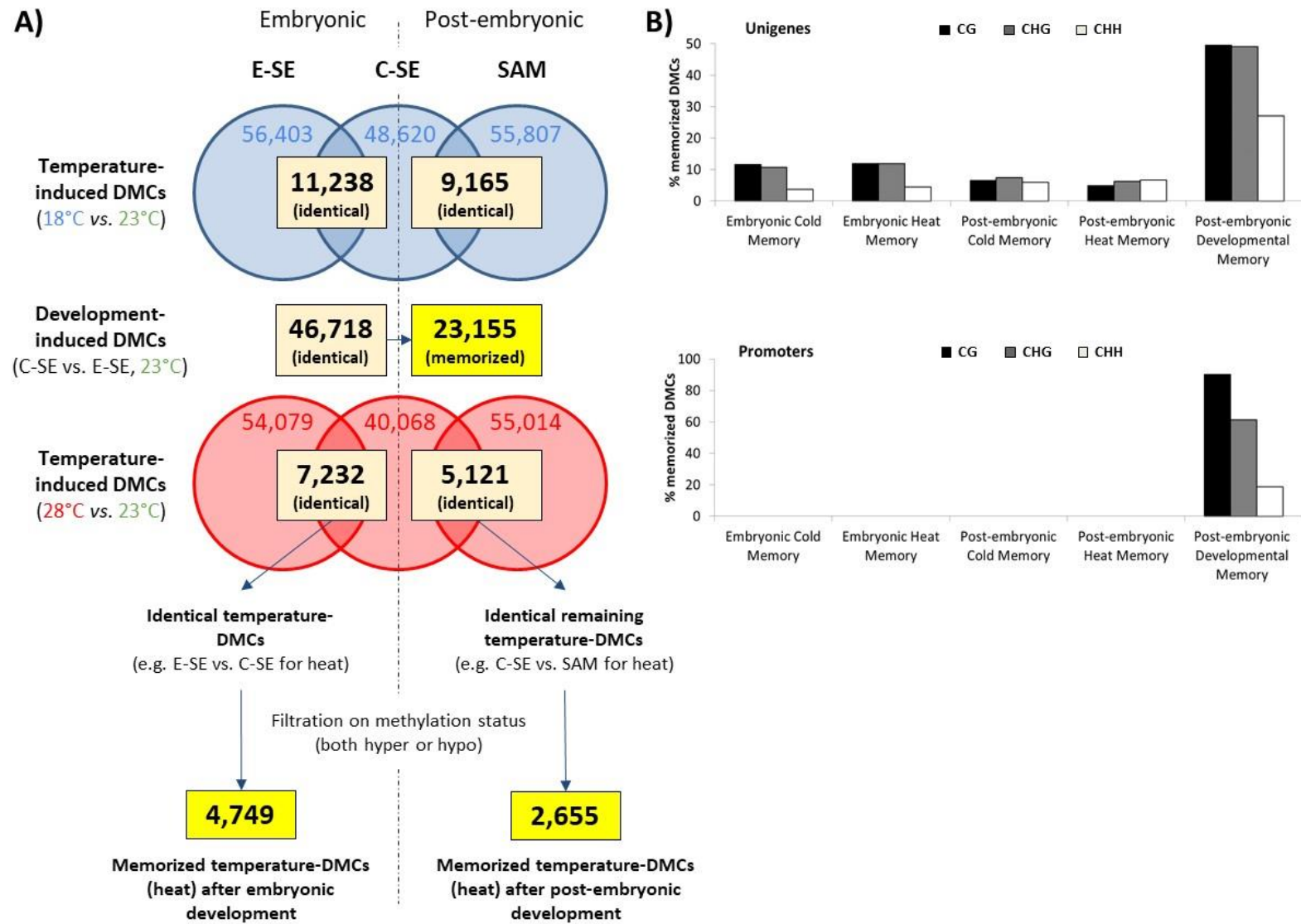
1233 **C-D.** Percentage of SMP sites in significant Differentially Methylated Cytosines (DMCs), i.e., with q -value < 0.01 and at least a 25% methylation
1234 difference, compared to the total number of SMP sites analyzed by cytosine context (CG, CHG, CHH) for all *P. pinaster* samples. **C.** Unigenes;
1235 **D.** Promoters. The different types of DMC (cold/heat temperature-, remaining temperature- and embryonic/post-embryonic development-DMC)
1236 are indicated (see Fig. S6).



1237

1238 **Figure 4:** Number of unigenes (left) and promoters (right) with Differentially Methylated Cytosines (DMCs) in the 3 contexts (CG, CHG, CHH).

- 1239 **A.** Temperature effect (seen in E-SE, C-SE) and remaining temperature effect (seen in SAM) following cold (18 vs. 23°C) and heat (28 vs. 23°C)
1240 treatments.
- 1241 **B.** Developmental effect (at 23°C) during embryonic (E-SE to C-SE) and post-embryonic development (C-SE to SAM).
- 1242 **C.** Temperature-induced memory during embryonic (E-SE to C-SE) and post-embryonic development (C-SE to SAM) following cold (18 vs. 23°C)
1243 and heat (28 vs. 23°C) treatments.



1244

1245 **Figure 5: Memory methylome.**

1246 **A.** Analysis flow chart to estimate the number of stable, memorized DMCs (highlighted in yellow) induced by temperature (cold: 18 vs. 23°C;
1247 heat: 28 vs. 23°C) or embryo development (C-SE vs. E-SE at 23°C) during maturation for unigenes in CG context.

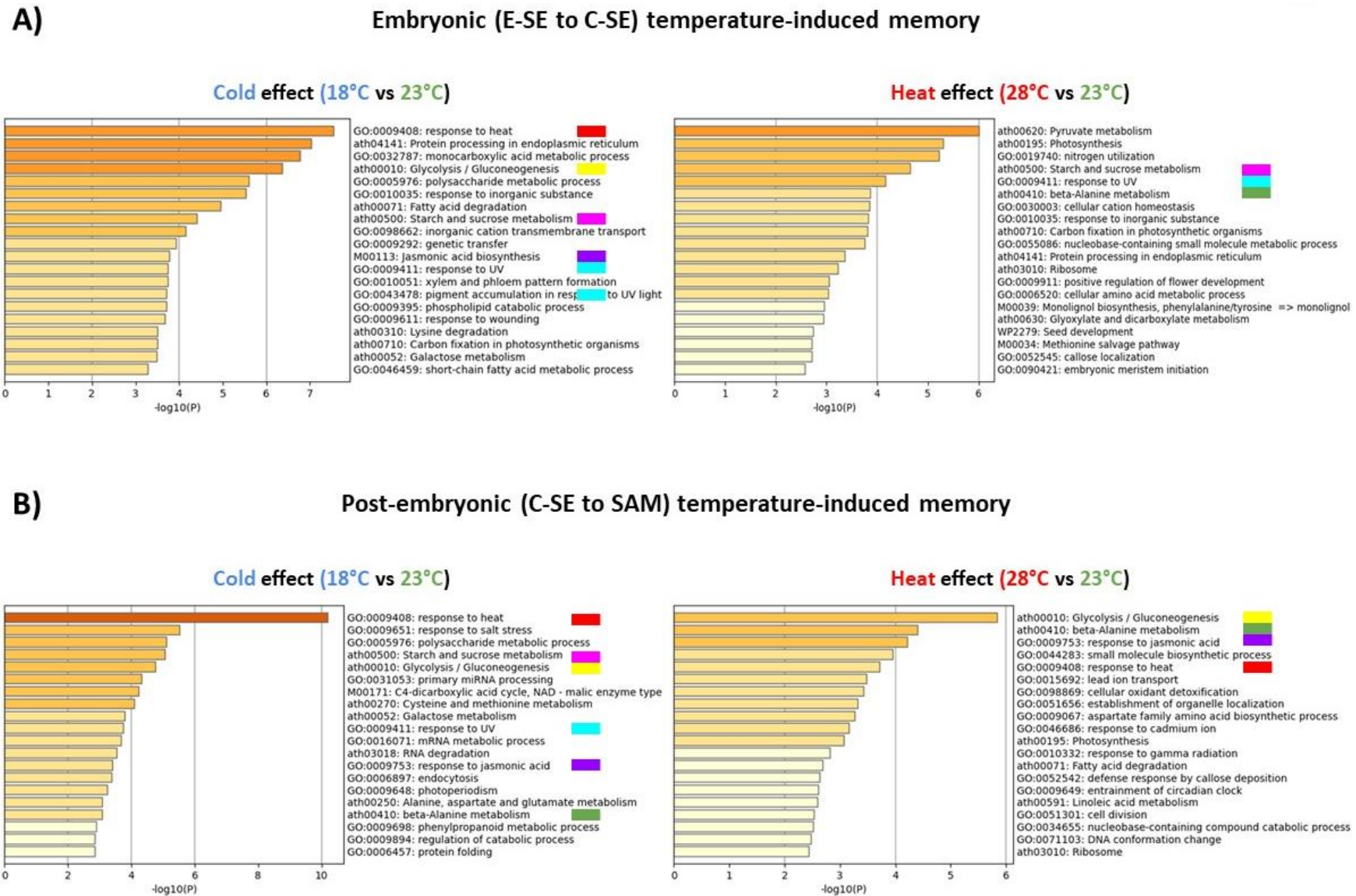
1248 We first calculated the number of identical DMCs, i.e., that are found at the same positions between different sample types:

1249 i) Temperature effect: number of identical DMCs induced by cold or heat comparing E-SE and C-SE (embryonic, temperature-DMCs) or C-SE
1250 and SAM (post-embryonic, remaining temperature-DMCs).

1251 ii) Development effect: number of identical DMCs induced by embryo development comparing C-SE (embryonic development-DMCs) and SAM
1252 (post-embryonic development-DMCs).

1253 Each category of identical temperature- or development-DMCs were then filtered for the same differential of hyper- or hypo-methylation to identify
1254 stable, memorized DMCs. We found e.g., 4,749 or 2,655 memorized heat-induced DMCs after embryonic or post-embryonic development,
1255 respectively, and 23,155 development-induced DMCs memorized after post-embryonic growth.

1256 **B.** Percentage (%) of memorized DMCs (all 3 contexts CG, CHG, CHH) in unigenes (up) or promoters (down) induced by temperature (cold: 18
1257 vs. 23°C; heat: 28 vs. 23°C) or embryo development (C-SE vs. E-SE at 23°C). Post-embryonic developmental memory and both embryonic and
1258 post-embryonic temperature-induced (cold or heat) memories are shown.



1259

1260

Figure 6: GO enrichment analysis of unigenes with memorized temperature-induced DMCs (memory) for all 3 contexts.

1261 **A.** Embryonic (E-SE to C-SE) development.

1262 **B.** Post-embryonic (C-SE to SAM) development.

1263 Most recurrent GO terms in at least 3 out of the 4 different cold (18/23°C) and heat (28/23°C) situations are highlighted by colored boxes:

1264 *Stress GO terms* related to response to heat (red), UV radiations (blue), jasmonic acid (purple), beta-alanine metabolism (green).

1265 *Metabolic GO terms* related to glycolysis /gluconeogenesis (yellow), starch and sucrose metabolism (pink).